*J. Fluid Mech.* (1978), *vol.* 84, *part* 2, *pp.* 209–235
*Printed in Great Britain*



# Free-stream turbulence near plane boundaries†

By J. C. R. HUNT

Department of Applied Mathematics and Theoretical Physics
and Department of Engineering, University of Cambridge

AND J. M. R. GRAHAM

Department of Aeronautics, Imperial College, London

(Received 22 September 1976 and in revised form 12 March 1977)

Grid turbulence convected by a free stream past a rigid surface moving at the same speed as the free stream is analysed by boundary-layer theory and spectral methods. The turbulence is assumed to be weak, i.e. $u'_\infty/\bar{u}_\infty \ll 1$, and its Reynolds number to be large, i.e. $u'_\infty L_\infty/\nu \gg 1$, where $u'_\infty$ is the r.m.s. turbulent velocity. Two regions are found to exist. The outer, source region $B^{(s)}$ has a thickness of the order of the integral scale $L_\infty$. Here the normal component of turbulence decreases and the lateral and streamwise components are amplified. The inner, viscous region $B^{(v)}$ has thickness $[x\nu/\bar{u}_\infty]^{\frac{1}{2}}$, where $x$, $\nu$ and $\bar{u}_\infty$ are the streamwise co-ordinate, kinematic viscosity and mean velocity respectively. Here the turbulent velocity decays to zero at the surface. Spectra variances and cross-correlations are calculated and found to compare well with measurements of turbulence near moving walls by Uzkan & Reynolds (1967) and Thomas & Hancock (1977).

The results of this theory are shown to have a number of applications including the prediction of turbulence near wind-tunnel walls and near flat plates placed parallel to the flow.

## 1. Introduction

A flat rigid surface introduced into a unidirectional turbulent shear flow affects the turbulence by means of two mechanisms. First, the no-slip condition at the surface produces a mean velocity gradient which interacts with the velocity and the vorticity of the turbulence. Second, the velocity fluctuations of the turbulence must be zero at the wall.

Most calculation methods for turbulent flows are exclusively concerned with the first effect, which can be analysed and physically explained in terms of the energy transfer between the mean and turbulent flow fields, hence its obvious practical importance. This paper is exclusively concerned with the second mechanism, which does not lead to significant changes in the energy of the mean flow and cannot usefully be considered by energy arguments. However changes due to the second mechanism are of practical importance.

A critical experiment to examine this particular interaction between turbulence and a fixed surface without the interference of a mean velocity boundary layer is to study

† Main conclusions of this work were presented by J. C. R. Hunt at the University of Southampton Colloquium on Coherent Structures in Turbulence in March 1974.

grid turbulence near a moving wall. Such an experiment was first conceived and performed by Uzkan & Reynolds (1967) in a small water channel. More recently it has been repeated in a large wind tunnel by Thomas & Hancock (1977).

In this paper we develop a theory for this experiment and calculate the changes in the variances, spectra, cross-spectra and cross-correlations of weak homogeneous free-stream turbulence near a flat surface moving with the same mean speed as the free stream. The analysis and statistical methods used are similar to those developed by Hunt (1973) and Graham (1976) for turbulent flows round bluff bodies. In the limit of large Reynolds number a moving wall or a bluff body acts like a sheet of random sources producing an irrotational flow field such that the net normal velocity is zero at the surface. The moving-wall problem is *simpler* than the bluff-body problem because there is no change in the mean velocity. Therefore no distortion of the vorticity of the turbulence occurs and no *inviscid rotational* flow field is created. Sufficiently close to the moving surface a rotational fluctuating flow field must exist as the *fluctuating* velocity is brought to zero.

Irrotational velocity fluctuations are, of course, a well-known feature of turbulent flows near rigid surfaces. For example they exist outside a turbulent boundary layer, being driven by the rotational motions in the boundary layer (Phillips 1955). On the other hand, in the inner part of a turbulent boundary layer there are large-scale, relatively low frequency motions driven by the large eddies in the outer part of the boundary layer. These have been described as 'inactive motions' by Townsend (1961, 1976) and Bradshaw (1967), who observed that they are partly made up of irrotational motions. But they did not develop any method for calculating these motions, nor did they discuss how these motions are brought to rest at the wall.

The main object of this paper is to provide a theory for comparison with the experimental results of Uzkan & Reynolds (1967) and Thomas & Hancock (1977). The application of this analysis to 'inactive' motions in boundary layers and the distortion near rigid wind-tunnel walls of large-scale turbulence generated by grids or other devices will be discussed in later papers.

## 2. A theory of homogeneous turbulence near a moving wall

### 2.1. *Assumptions and equations*

Consider the idealized flow depicted in figure 1, in which weak homogeneous turbulence swept along by a stream with mean velocity $\bar{u}_\infty$ is suddenly brought into contact with a rigid surface $y = 0$, $x > 0$ also moving at speed $\bar{u}_\infty$. The object of the analysis is to demonstrate how this surface affects the turbulence.

Initial conditions are necessary to determine the flow and it is assumed that a homogeneous, statistically stationary *vorticity* field, created by an idealized grid at $x_g$, meets the wall at $x = 0$. (Downstream the flow near the wall turns out to be quite sensitive to the initial conditions, which must therefore be specified precisely.) Various means of more or less approximately achieving this situation are discussed later.

A formal statement of the problem is that we have to solve

$$\partial \mathbf{u}^*/\partial t + (\mathbf{u}^*.\nabla)\,\mathbf{u}^* = -\rho^{-1}\nabla p + \nu\nabla^2\mathbf{u}^*, \tag{2.1}$$

$$\nabla.\mathbf{u}^* = 0, \tag{2.2}$$

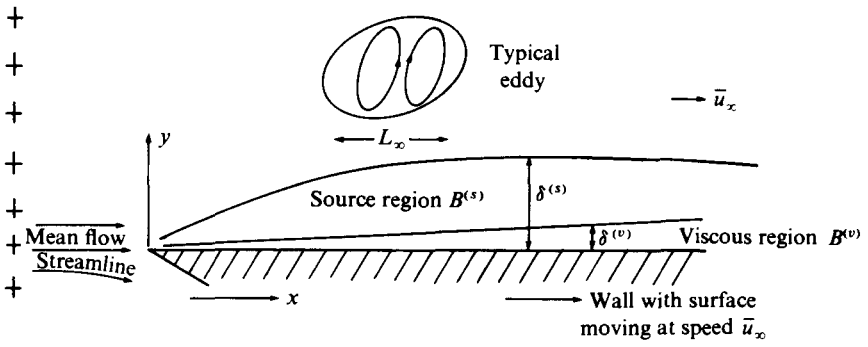


FIGURE 1. Definition sketch showing the upstream grid, the moving wall, the source region $B^{(s)}$ and the viscous region $B^{(v)}$.

where $\mathbf{u}^*$, $p$, $\rho$ and $\nu$ are the velocity, pressure, density and kinematic viscosity respectively. Let $\boldsymbol{\omega}^*$ be the vorticity $\nabla \times \mathbf{u}^*$. Then on expressing $\mathbf{u}^*$ and $\boldsymbol{\omega}^*$ in terms of their mean and fluctuating components, we get

$$\mathbf{u}^* = \bar{\mathbf{u}}(\mathbf{x}) + \mathbf{u}'(\mathbf{x}, t), \quad \boldsymbol{\omega}^* = \bar{\boldsymbol{\omega}}(\mathbf{x}) + \boldsymbol{\omega}'(\mathbf{x}, t),$$

where an overbar denotes a time or ensemble mean. The boundary conditions are

$$\bar{\mathbf{u}} = (\bar{\mathbf{u}}_\infty, 0, 0) \quad \begin{cases} \text{on } y = 0, \quad 0 < x < \infty, & (2.3a) \\ \text{as } x \to -\infty, & (2.3b) \end{cases}$$

where $\bar{u}_\infty$ is a constant equal to the upstream velocity and the speed of the moving floor. A specified vorticity field $\boldsymbol{\omega}_0'$ is created upstream, so that

$$\boldsymbol{\omega}' = \boldsymbol{\omega}_0'(x_0, y, z, t) \quad \text{at} \quad x = x_0, \quad \text{far upstream of } x = 0. \tag{2.4a}$$

No velocity fluctuations are assumed to exist on the moving wall, so that

$$\mathbf{u}' = 0 \quad \text{on} \quad y = 0, \quad 0 < x < \infty. \tag{2.4b}$$

The following assumptions are made about the intensity and scale (or Reynolds number) of the turbulence:

$$\alpha = u_\infty'/\bar{u}_\infty \ll 1, \quad u_\infty' L_\infty/\nu \gg 1, \tag{2.5), (2.6}$$

where $u_\infty' \equiv [\overline{(u_{\infty 1}')^2}]^{\frac{1}{2}}$ is the root mean square of the $x$ or longitudinal fluctuating velocity component $u_1'$ and $L_\infty$ is the integral scale of $u_1'$, both being defined at $x = 0$.

From the assumption of weak turbulence (2.5), the solution to (2.1) and (2.2) for the mean velocity $\bar{\mathbf{u}}(\mathbf{x})$ in the limit $\alpha \to 0$ is

$$\bar{\mathbf{u}}(\mathbf{x}) = (\bar{u}_\infty, 0, 0). \tag{2.7}$$

Substituting (2.7) into (2.1) and using the assumptions (2.5) and (2.6), the equations for $\mathbf{u}'$ and the fluctuating vorticity $\boldsymbol{\omega}'$ become

$$\frac{\partial \mathbf{u}'}{\partial t} + \bar{u}_\infty \frac{\partial \mathbf{u}'}{\partial x} = \frac{d\mathbf{u}'}{\partial t} = -\frac{1}{\rho}\nabla p' + \nu \nabla^2 \mathbf{u}' + O((u_\infty')^2/L_\infty), \tag{2.8}$$

$$\frac{\partial \boldsymbol{\omega}'}{\partial t} + \bar{u}_\infty \frac{\partial \boldsymbol{\omega}'}{\partial x} = \frac{d\boldsymbol{\omega}'}{dt} = \nu \nabla^2 \boldsymbol{\omega}' + O((u_\infty')^2/L_\infty^2), \tag{2.9}$$

where the order-of-magnitude estimates are for the fluctuating nonlinear terms since the scale of the energy-containing eddies is of the order of $L_\infty$. Under assumption (2.5), these terms are small compared with terms on the left-hand side of the equations. If assumption (2.6) is made also, (2.8) or (2.9) implies that in the absence of any boundaries the *time scale* for the variation of the velocity of any fluid element is of the order of $L_\infty/u'$, sometimes known as the 'turnover time', or the Lagrangian time scale (Tennekes & Lumley 1972). This time corresponds to a distance along the flow of $L_\infty \bar{u}/u' = \mathscr{L}_L$, a turnover distance. Equations (2.8) and (2.9) also imply that for eddy scales (or wavelengths of Fourier components) of the order of $L_\infty$ the viscous terms are negligible if the Reynolds number of the turbulence is large enough, i.e. under assumption (2.6). But over a distance of order $\mathscr{L}_L$ the viscous stresses acting on the smallest scales produce large changes in the energy-containing eddies. Thus over a distance $x - x_0$ small compared with $\mathscr{L}_L$ the velocity and vorticity of fluid elements far from any boundary do not change from their values at $x_0$ as the elements are convected: they are 'frozen'. Therefore over distances $0 < x - x_0 \ll \mathscr{L}_L$ in the free stream,

$$d\boldsymbol{\omega}'_\infty/dt = 0, \quad d\mathbf{u}'_\infty/dt = 0 \quad \text{for all} \quad x_0 > O(L_\infty). \tag{2.10}$$

Thence the outer boundary conditions on the turbulence in the region near the wall are

$$\left.\begin{aligned} \boldsymbol{\omega}'(\mathbf{x},t) &\to \boldsymbol{\omega}'_\infty(\mathbf{x},t) = \boldsymbol{\omega}'_0(x_0,y,z,t-x/\bar{u}_\infty) \\ \mathbf{u}'(x,t) &\to \mathbf{u}'_\infty(\mathbf{x},t) = \mathbf{u}'_0(x_0,y,z,t-x/\bar{u}_\infty) \end{aligned}\right\} \quad \text{as } y \to \infty, \tag{2.11, 2.12}$$

where $\boldsymbol{\omega}'_0$ and $\mathbf{u}'_0$ are the fluctuating vorticity and velocity created by the grid. $\boldsymbol{\omega}'_0$ and $\mathbf{u}'_0$ are assumed to be statistically homogeneous in the $y$ and $z$ directions.

The effect of the wall on this free-stream turbulence is to produce two distinct boundary layers $B^{(v)}$ and $B^{(s)}$, which we first discuss qualitatively to explain the direction of the formal asymptotic analysis. Since $u'_1 = u'_3 = 0$ on $y = 0$, $\omega'_2 = 0$ on $y = 0$, and a boundary layer must exist for the fluctuating vorticity. Equation (2.9) suggests that this has a thickness $\delta^{(v)} \sim (\nu x/\bar{u}_\infty)^{\frac{1}{2}}$, if $\delta^{(v)}$ is small compared with a typical eddy size $L_\infty$. Thus a change in $\mathbf{u}'$ must occur across $B^{(v)}$. But since $u'_i = 0$ on $y = 0$, the continuity equation requires that just outside $B^{(v)}$, at $y = \delta^{(v)}$, $u'_2 \sim \delta^{(v)} u'_1/x$. Consequently, even if $u'_1 \sim u'_{\infty 1}$, it is not possible for the normal component of velocity $u'_2$ to be restored to its upstream or far-field value just above the viscous boundary layer. This change must occur in a deeper layer through which $u'_2$ increases from approximately zero at $y = \delta^{(v)}$ to its far-field value $u'_{\infty 2}$ at $y = \delta^{(s)}$. The difference between the velocity field in this layer and that in the far field can be regarded as being produced by a source-like distribution $-u'_{\infty 2}$ on the wall. Hence we term this layer the source boundary layer $B^{(s)}$.

### 2.2. *The viscous and source layers*

For the analysis of $B^{(v)}$ we use the non-dimensional co-ordinates

$$X = x/L_\infty, \quad \eta = y/[L_\infty \nu/\bar{u}_\infty]^{\frac{1}{2}}, \quad Z = z/L_\infty, \quad T = t\bar{u}_\infty/L_\infty \tag{2.13}$$

and in $B^{(s)}$ the definitions $X$, $Z$ and $T$ are unchanged while $Y = y/L_\infty$. We shall also use assumptions (2.5) and (2.6). The non-dimensional flow variables are

$$\omega_i = \omega'_i L_\infty/u'_\infty, \quad u_i = u'_i/u'_\infty, \quad p = p'/(\rho \bar{u}_\infty u'_\infty), \tag{2.14}$$

which are conveniently expressed as sums of different terms associated with $B^{(v)}$ and $B^{(s)}$:

$$\left.\begin{aligned}\omega_i &= \omega_{\infty i}(\mathbf{X},T)+\omega_i^{(s)}(\mathbf{X},T)+\omega_i^{(v)}(\mathbf{X},\eta,Z,T),\\ u_i &= u_{\infty i}(\mathbf{X},T)+u_i^{(s)}(\mathbf{X},T)+u_i^{(v)}(\mathbf{X},\eta,Z,T).\end{aligned}\right\} \tag{2.15}$$

All the non-dimensional terms in (2.15) are assumed to be $O(1)$, and $\mathbf{X} = (X, Y, Z)$.

The equations for the two layers follow from the above scaling, the Navier–Stokes equations (2.1) and (2.2), and the results already obtained for $\mathbf{u}'_\infty$ and $\boldsymbol{\omega}'_\infty$ in (2.12) and (2.11). Thus, ignoring terms $O(R^{-\frac{1}{2}})$ and smaller, we find that in $B^{(s)}$

$$\frac{\partial u_i^{(s)}}{\partial T}+\frac{\partial u_i^{(s)}}{\partial X}=-\frac{\partial p}{\partial X_i},\quad \frac{\partial u_i^{(s)}}{\partial X_i}=0, \tag{2.16a, b}$$

$$(\partial/\partial T+\partial/\partial X)(\omega_{\infty i}+\omega_i^{(s)})=0, \tag{2.17}$$

where $X_i$ is the $i$th component of $\mathbf{x}$, and in $B^{(v)}$

$$\left(\frac{\partial}{\partial T}+\frac{\partial}{\partial X}\right)\begin{pmatrix}u_1^{(s)}+u_1^{(v)}\\ u_3^{(s)}+u_3^{(v)}\\ u_2^{(s)}+u_2^{(v)}\end{pmatrix}=-\begin{Bmatrix}\partial p/\partial X\\ \partial p/\partial Z\\ R^{\frac{1}{2}}\,\partial p/\partial\eta\end{Bmatrix}+\frac{\partial^2}{\partial\eta^2}\begin{Bmatrix}u_1\\ u_3\\ u_2\end{Bmatrix}, \tag{2.18}$$

$$\frac{\partial u_1^{(v)}}{\partial X}+R^{\frac{1}{2}}\frac{\partial u_2^{(v)}}{\partial\eta}+\frac{\partial u_3^{(v)}}{\partial Z}=0, \tag{2.19}$$

$$\left(\frac{\partial}{\partial T}+\frac{\partial}{\partial X}\right)\omega_i^{(v)}+\omega_i^{(s)}=\frac{\partial^2\omega_i}{\partial\eta^2}. \tag{2.20}$$

The boundary conditions on $u_i^{(s)}$, $u_i^{(v)}$, $\omega_i^{(s)}$ and $\omega_i^{(v)}$ are

$$\omega_i^{(s)}+\omega_i^{(v)}=0 \quad \text{as} \quad x\to\infty \quad [\text{from (2.11) and (2.4}a)], \tag{2.21}$$

$$u_i^{(s)}+u_i^{(v)}=-u_{\infty i} \quad \text{on} \quad y=0,\quad x\geqslant 0 \quad [\text{from (2.4)}], \tag{2.22}$$

$$\omega_i^{(s)}+\omega_i^{(v)}\to 0,\quad u_i^{(s)}+u_i^{(v)}\to 0 \quad \text{as} \quad y\to\infty \quad [\text{from (2.10)}]. \tag{2.23}$$

The variables $u_i^{(v)}$ and $\omega_i^{(v)}$ are chosen to be zero outside the viscous boundary layer. Therefore the last boundary condition is replaced by

$$\omega_i^{(v)}\to 0,\quad u_i^{(v)}\to 0 \quad \text{as} \quad \eta\to\infty, \tag{2.24a}$$

$$\omega_i^{(s)}\to 0,\quad u_i^{(s)}\to 0 \quad \text{as} \quad Y\to\infty. \tag{2.24b}$$

The solution to (2.17) subject to (2.21), (2.24$a$) and (2.11) is

$$\omega_i^{(s)}=0, \tag{2.25}$$

which means that in our problem the vorticity is the same in $B^{(s)}$ as in the outer flow. It is not possible to calculate $u_i^{(s)}$ until the boundary conditions are known on $Y=0$. This requires studying $B^{(v)}$, where the simplest variable to calculate is $\omega_2^{(v)}$.

*Solution for $B^{(v)}$.* Since $u_3 = u_1 = 0$ at $y$

$$\omega_2^{(v)}(X,\eta=0,Z,T)=-\omega_\infty(X,y=0,Z,T)=-\omega_0(0,Y=0,Z,T-X). \tag{2.24c}$$

The equation for $\omega_2^{(v)}$ is

$$\left(\frac{\partial}{\partial T}+\frac{\partial}{\partial X}\right)\omega_2^{(v)}=\frac{\partial^2\omega_2^{(v)}}{\partial\eta^2}.$$

Thus to satisfy (2.24*a*, *c*) the solution must be

$$\omega_2^{(v)} = -\omega_0(0, Y = 0, Z, T - X)\,\mathrm{erfc}\{\eta/(4X)^{\frac{1}{2}}\}. \tag{2.26}$$

Thus we conclude that $B^{(v)}$ has the form of a growing boundary layer with thickness

$$\delta^{(v)} \simeq 4(x\nu/\bar{u}_\infty)^{\frac{1}{2}}. \tag{2.27}$$

$\omega_1^{(v)}$ and $\omega_3^{(v)}$ cannot be calculated at this stage because the derivatives of $u_1^{(v)}$ at $y = 0$, which are needed to specify $\omega_1^{(v)}$ and $\omega_3^{(v)}$ at $y = 0$, are not yet known. However, having shown that $B^{(v)}$ has a boundary-layer structure, at least for one component of vorticity, it is now reasonable to make the usual boundary-layer approximations for $u_i^{(v)}$. These can be checked *a posteriori*.

From (2.18), we have $\partial p/\partial\eta = 0$, whence

$$\frac{\partial}{\partial\eta}\left(\frac{\partial p}{\partial X}\right) = \frac{\partial}{\partial\eta}\left(\frac{\partial p}{\partial Z}\right) = 0 \quad \text{in} \quad B^{(v)}.$$

Therefore in $B^{(v)}$, $\partial p/\partial X$ and $\partial p/\partial Z$ are determined by their values in $B^{(s)}$ as $Y \to 0$, which are given by (2.16). Substituting these expressions into (2.18) gives

$$\left(\frac{\partial}{\partial T} + \frac{\partial}{\partial X}\right) u_j^{(v)} = \frac{\partial^2}{\partial\eta^2} u_j^{(v)} \quad (j = 1, 3), \tag{2.28}$$

where $$u_j^{(v)} \to 0 \quad \text{as} \quad \eta \to \infty$$

and $$u_j^{(v)} = -(u_{\infty j} + u_j^{(s)})(X, Y = 0, Z, T) \quad \text{at} \quad \eta = 0 \Big\} \quad (j = 1, 3).$$

Although $u_1^{(v)}$ and $u_3^{(v)}$ cannot be found until we know the $u_i^{(s)}$, we see that $u_1^{(v)}$ and $u_3^{(v)}$ have typical boundary-layer profiles decaying to zero at a value of $\eta$ approximately given by (2.27).

$u_2^{(v)}$ can be found in terms of $u_1^{(v)}$ and $u_3^{(v)}$ from the continuity equation (2.19), from which we see that, since $u_2^{(v)} \to 0$ as $\eta \to \infty$,

$$u_2^{(v)} = 0 \quad \text{in} \quad B^{(v)}. \tag{2.29}$$

(In fact $u_2^{(v)} = O(R^{-\frac{1}{2}}\bar{u}_\infty)$, but we are ignoring terms of this order.) Then applying the boundary condition (2.22) gives

$$u_2^{(s)}(X, Y = 0, Z, T) = -u_{\infty 2}(X, Y = 0, Z, T). \tag{2.30}$$

The fact that (2.30) specifies $u_2^{(s)}$ on $Y = 0$ now enables us to calculate $u_i^{(s)}$ throughout $B^{(s)}$. Since $\omega_i^{(s)} = 0$ [see (2.25)] we express $\mathbf{u}^{(s)}$ as

$$\mathbf{u}^{(s)} = -\nabla\Phi(\mathbf{X}, T), \tag{2.31}$$

and since $\nabla.\mathbf{u}^{(s)} = 0$ it follows that

$$\nabla^2\Phi = 0. \tag{2.32}$$

The boundary conditions on $\Phi$ follow from (2.31), (2.30) and (2.24*b*), namely

$$\left.\begin{aligned} \partial\Phi/\partial Y = u_{\infty 2}(X, Y = 0, Z, T) \quad \text{on} \quad Y = 0, \quad X > 0, \\ \nabla\Phi \to 0 \quad \text{as} \quad Y \to \infty. \end{aligned}\right\} \tag{2.33a}$$

If the mean flow is so arranged that the mean streamline which meets the surface of the wall $Y = 0$, $X \geqslant 0$ also lies approximately along $Y = 0$ upstream of the wall, as shown in figure 1, then the flow field for $Y \geqslant 0$ is similar to that for flow past an

idealized thin flat plate intersecting the turbulent flow with its leading edge at $X = 0$, $Y = 0$. In such a case, which is approximately the situation for the experiments of Thomas & Hancock (1977), the flat-plate experiments of § 3.3 and possibly the experiments of Uzkan & Reynolds (1967), the appropriate upstream boundary condition is

$$\Phi = 0 \quad \text{on} \quad Y = 0, \quad X < 0. \tag{2.33b}$$

On the other hand if the wall extends continuously up to and beyond the grid and no attempt is made to remove the wall layer coming off the grid as in the experiments of Cooke (1971) and Petty (unpublished), $\partial\Phi/\partial Y$ becomes a function of $X$, $Z$ and $T$ on $Y = 0$ which is difficult to specify in the region of the grid but which rapidly decreases to zero upstream of the grid, within a distance of order $L_\infty$.

However if the turbulence is to be analysed at a station $X$ sufficiently far downstream of $X = 0$, the upstream boundary condition becomes immaterial and the solution of (2.32) with (2.33*a*) is

$$\Phi(X, Y, Z, T) = -\frac{1}{2\pi}\int_0^\infty \int_{-\infty}^\infty \frac{u_{\infty 2}(X', Y' = 0, Z', T)\, dX'\, dZ'}{[(X-X')^2 + Y^2 + (Z-Z')^2]^{\frac{1}{2}}}. \tag{2.34}$$

This solution is correct except within distances of order $L_\infty$ from $X = 0$, for which the full solution with boundary condition (2.33*b*) is given in appendix A. The full solution shows that the leading-edge contribution becomes negligible for $X \gtrsim 1$. (For further justification see § 2.3.) Given $\Phi(\mathbf{X}, T)$, $\mathbf{u}^{(s)}$ can be calculated from (2.31) throughout $B^{(s)}$ in terms of $u_{\infty 2}(\mathbf{X}, T)$. In particular $u_1^{(s)}$ and $u_3^{(s)}$ at $Y = 0$ can be found, so that $u_1^{(v)}$ and $u_3^{(v)}$ can be calculated from (2.28).

In the limit $X \to \infty$, it follows from (2.12) that (2.34) can be rewritten as

$$\frac{\partial\Phi}{\partial X}(Y = 0) = \int_0^\infty \int_{-\infty}^\infty \frac{u_{\infty 2}(0, 0, Z', T - X + X'')\, dX''\, dZ'}{[X''^2 + (Z-Z')^2]^{\frac{3}{2}}}. \tag{2.35}$$

Thus for $X$ large enough, $u_1^{(s)}$ as $Y \to 0$ is a function of $T - X$ and $Z$ only, so that $u_{\infty 1} + u_1^{(s)}$ and, by similar arguments, $u_{\infty 3} + u_3^{(s)}$ can be written as

$$\left.\begin{aligned} u_{\infty 1}(X, 0, Z, T) + u_1^{(s)}(X, 0, Z, T) &= \mathscr{U}_1(Z, T - X) \\ u_{\infty 3}(X, 0, Z, T) + u_3^{(s)}(X, 0, Z, T) &= \mathscr{U}_3(Z, T - X) \end{aligned}\right\} \text{ when } X \to \infty. \tag{2.36}$$

Thence the appropriate solutions for $u_1^{(v)}$ and $u_3^{(v)}$ in (2.28) are

$$u_1^{(v)} = -\mathscr{U}_1(Z, T - X)\operatorname{erfc}\{\eta/(4X)^{\frac{1}{2}}\}, \quad u_3^{(v)} = \mathscr{U}_3(Z, T - X)\operatorname{erfc}\{\eta/(4X)^{\frac{1}{2}}\}. \tag{2.37a}$$

Thus the thickness $\delta^{(v)}$ of the region $B^{(v)}$, defined as the value of $y$ at which $u_1$ is 99 % of its value in $B^{(s)}$ as $Y \to 0$, is given by

$$\delta^{(v)} = 4{\cdot}0(xv/\bar{u}_\infty)^{\frac{1}{2}}. \tag{2.37b}$$

### 2.3. *Fourier analysis of* $B^{(s)}$

Using the same notation as in the paper of Hunt (1973), the normalized turbulent velocity $\mathbf{u}$ is expressed in terms of two- or three-dimensional Fourier transforms. Near the wall, where the velocity is only homogeneous in $z$ and $t$,

$$\begin{Bmatrix} u_i(\mathbf{X}, t) \\ \Phi(\mathbf{X}, t) \end{Bmatrix} = \int_{-\infty}^\infty \int_{-\infty}^\infty \begin{Bmatrix} \hat{\mathbf{u}} \\ \hat{\Phi} \end{Bmatrix}(K_1, K_3; X, Y) \exp\{i(-K_1 T + K_3 Z)\}\, dK_1\, dK_3. \tag{2.38}$$

But in the free stream, where the turbulence is homogeneous in $x$, $y$ and $z$ and is convected, i.e. 'frozen', by the mean flow,

$$u_{\infty i}(\mathbf{X},t) = \iiint_{-\infty}^{\infty} \mathscr{S}_{\infty i}(K_1,K_2,K_3)\exp\{i(-K_1 T + K_1 X + K_2 Y + K_3 Z)\}\,dK_1\,dK_2\,dK_3. \tag{2.39}$$

$\mathbf{K}$ is a non-dimensional wavenumber defined in terms of the dimensional wavenumber $\mathbf{K}^*$ as

$$\mathbf{K} = \mathbf{K}^* L_\infty, \tag{2.40}$$

so that $K_1$ is effectively a non-dimensional frequency ($= 2\pi n L_\infty/\bar{u}_\infty$) corresponding to an oscillation with frequency $n$.

In order to express the turbulence near the wall in terms of its spectrum in the free stream, we express $\hat{\hat{u}}_i$ and $\hat{\hat{\Phi}}$ in terms of $\mathscr{S}_{\infty i}$ by the equations

$$\begin{Bmatrix}\hat{\hat{u}}_i \\ \hat{\hat{\Phi}}\end{Bmatrix}(K_1,K_3;X_1\,Y) = \int_{-\infty}^{\infty} \begin{Bmatrix}M_{il}(\mathbf{K};X,Y) \\ \beta_l(\mathbf{K};X,Y)\end{Bmatrix} \mathscr{S}_{\infty l}(\mathbf{K})\,dK_2, \tag{2.41}$$

which are similar to equations (4.20) in Hunt (1973). In region $B^{(s)}$ it is convenient to express the tensor $M_{il}$ in terms of two other terms as

$$M_{il} = M_{il}^{(\infty)} + M_{il}^{(S)},$$

where

$$M_{il}^{(\infty)} = \delta_{il}\exp\{i(K_1 X + K_2 Y)\} \tag{2.42a}$$

and since, from (2.31),

$$u_i = -\partial\Phi/\partial X_i,$$

$$M_{il}^{(S)} = (-\partial\beta_l/\partial X, -\partial\beta_l/\partial Y, -iK_3\beta_l). \tag{2.42b}$$

In Hunt (1973) it was necessary to add another tensor $M_{il}^{(d)}$ due to the distortion of the vortex lines by the variations of the mean flow around the bluff body.

Substituting (2.39) and (2.41) into (2.34), we find that when $x \gg 1$

$$\beta_1 = \beta_3 = 0 \tag{2.43a}$$

and

$$\beta_2(\mathbf{K};X,Y) = -\frac{1}{2\pi}\int_0^\infty \int_{-\infty}^{\infty} \frac{\exp\{i(K_1 X' + K_3(Z-Z'))\}}{[(X-X')^2 + Y^2 + (Z-Z')^2]^{\frac{1}{2}}}\,dX'dZ'. \tag{2.43b}$$

This double integral can be evaluated when $X \to \infty$ to give

$$\beta_2 = -\exp\{iK_1 X - (K_1^2+K_3^2)^{\frac{1}{2}} Y\}/(K_1^2+K_3^2)^{\frac{1}{2}} \quad \text{(Erdélyi } et\ al. \text{ 1954, pp. 11, 56).} \tag{2.44}$$

If we define $\Delta\beta$ as the difference between this asymptotic result for $\beta_2$ (at large $X$) and the expression for $\beta_2$ at arbitrary $X$, given in appendix A, then the extra contribution due to the influence of the 'leading edge' can be evaluated on $Y = 0$ as

$$\Delta\beta(X,0) = \frac{2\exp(iK_1 X)}{(K_1^2+K_3^2)^{\frac{1}{2}}}(1 - \operatorname{erf}\{[(iK_1+K_3)X]^{\frac{1}{2}}\}). \tag{2.45}$$

This can be expanded for large values of $X$ to give

$$\Delta\beta(X,0) = \frac{2}{\pi^{\frac{1}{2}}}\frac{\exp(-|K_3|X)(K_3 - iK_1)^{\frac{1}{2}}}{K_1^2+K_3^2} X^{-\frac{1}{2}} + O(\exp(-|K_3|X)\,X^{-\frac{3}{2}}), \tag{2.46}$$

which tends to zero as $X$ goes to infinity, but more slowly for very wide eddies (small $K_3$). However for the bulk of the energy-containing eddies with dimensions of order $L_\infty$, when $x \gtrsim L_\infty$ the leading-edge contribution $\Delta\beta \simeq 0$, so that $\beta_2$ is as given in (2.44).

On the plane $X = 0$, $\beta$ is continuous. But at $X = 0$, $Y = 0$ there is a square-root singularity in $\partial\beta/\partial X$, which is to be expected on account of the discontinuity at $X = 0$ in the singularity distribution on $Y = 0$.

From (2.45), (2.44) and (2.42), it follows that, in region $B^{(s)}$, when $\mathscr{L}_L \gg x \gtrsim L_\infty$

$$M_{i1} = \delta_{i1} \exp\{i(K_1 X + K_2 Y)\}, \quad M_{i3} = \delta_{i3} \exp\{i(K_1 X + K_2 Y)\}, \tag{2.47}$$

$$M_{i2} = \delta_{i2} \exp\{i(K_1 X + K_2 Y)\} + \left[\frac{iK_1}{(K_1^2+K_3^2)^{\frac{1}{2}}}, -1, \frac{iK_3}{(K_1^2+K_3^2)^{\frac{1}{2}}}\right] \times \exp\{iK_1 X - (K_1^2+K_3^2)^{\frac{1}{2}} Y\}. \tag{2.48}$$

### 2.4. *Calculation of spectra and variances in $B^{(s)}$*

For a homogeneous flow the three-dimensional Fourier transform $\mathscr{S}_{\infty i}$ of a turbulent velocity component $u_{\infty i}$ is related to the three-dimensional spectrum $\Phi_{\infty ij}(\mathbf{K})$. This relation can be used for the free-stream turbulence only when it is effectively homogeneous, i.e. when it has been convected several integral scales from the grid. Thus, when $x \gg L_\infty$ and the Fourier transforms of $u_{\infty i}$ are defined within a box with sides having lengths $L_\infty \mathscr{X}$, $L_\infty \mathscr{Y}$ and $L_\infty \mathscr{Z}$, we have

$$\overline{\mathscr{S}^\dagger_{\infty i}(K_1, K_2, K_3)\, \mathscr{S}_{\infty j}(K_1, K_2', K_3)} = [(\mathscr{X}\mathscr{Z})/\pi^2]\, \delta(K_2 - K_2')\, \Phi_{\infty ij}(\mathbf{K}), \tag{2.49}$$

where the dagger superscript denotes the complex conjugate [Hunt 1973, equation (3.34)]. Thence using (2.41) to express $u_i$ in terms of $\mathscr{S}_{\infty i}$, and integrating with respect to $K_2$ and $K_3$, the normalized one-dimensional cross-spectrum for the velocities at two points $\mathbf{X}_a = (X_a, Y_a, Z_a)$ and $\mathbf{X}_b = (X_b, Y_b, Z_b)$ is found in terms of the normalized three-dimensional spectrum of the free stream [as in Hunt 1973, equations (3.36), (3.32)]:

$$\Theta_{ij}(\mathbf{X}_a, \mathbf{X}_b; K_1) = \int_{-\infty}^{\infty}\int_{-\infty}^{\infty} M^\dagger_{il}(X_a, Y_a; \mathbf{K})\, M_{jm}(X_b, Y_b, \mathbf{K}) \exp\{iK_3(Z_a - Z_b)\} \times \Phi_{\infty lm}(\mathbf{K})\, dK_2\, dK_3, \tag{2.50}$$

where the definition of $\Theta_{ij}$ is

$$\Theta_{ij}(\mathbf{X}_a, \mathbf{X}_b; K_1) = \Theta^*_{ij}(\ddot{\mathbf{x}}_a, \ddot{\mathbf{x}}_b; K_1^*)/[(u'_\infty)^2 L_\infty]$$

and

$$\Theta^*_{ij}(\mathbf{x}_a, \mathbf{x}_b; K_1^*) = \frac{\bar{u}_\infty}{2\pi}\int_{-\infty}^{\infty} \overline{u'_i(\mathbf{x}, t)\, u'_j(\mathbf{x}, t+\tau)} \exp(-iK_1^* \tau \bar{u}_\infty)\, d\tau. \tag{2.51}$$

Substituting the results (2.47) and (2.48) for $M_{il}$ when $x \gg L_\infty$ into (2.50), we find that in region $B^{(s)}$ the cross-spectrum $\Theta_{11}$ is given by

$$\Theta_{11}(\mathbf{X}_a, \mathbf{X}_b; K_1) = \Theta_{\infty 11}(K_1) + I_{AC} + I_{BC}, \tag{2.52a}$$

where

$$I_{AC} = \int_{-\infty}^{\infty}\int_{-\infty}^{\infty} \frac{iK_1}{(K_1^2+K_3^2)^{\frac{1}{2}}} \exp\{i[(K_1 X_b - K_1 X_a) + K_3(Z_b - Z_a)]\} \exp\{-(K_1^2+K_3^2)^{\frac{1}{2}} Y\} \times [\exp\{-(K_1^2+K_3^2)^{\frac{1}{2}} Y_b\} \exp(-iK_2 Y_a)\, \Phi_{\infty 12} - \exp\{-(K_1^2+K_3^2)^{\frac{1}{2}} Y_a\} \times \exp(iK_2 Y_b)\, \Phi_{\infty 21}]\, dK_2\, dK_3, \tag{2.52b}$$

which is the contribution from three-dimensional cross-spectra between $u_{\infty 1}$ and $u_{\infty 2}$. Such a cross-spectrum exists in homogeneous turbulence because, even though $\overline{u_{\infty 1}(\mathbf{X})\, u_{\infty 2}(\mathbf{X})} = 0$, $\overline{u_{\infty 1}(\mathbf{X})\, u_{\infty 2}(\mathbf{X}+\mathbf{r})} \neq 0$ when $\mathbf{r} \neq 0$. The other integral in (2.52*a*) is

$$I_{BC} = \int_{-\infty}^{\infty}\int_{-\infty}^{\infty} \frac{K_1^2}{K_1^2+K_3^2} \exp\{i[K_1(X_b-X_a)+K_3(Z_b-Z_a)] - (K_1^2+K_3^2)^{\frac{1}{2}}(Y_b+Y_a)\} \times \Phi_{\infty 22}\, dK_2\, dK_3, \quad (2.52c)$$

which is the contribution to $\Theta_{11}$ solely from $u_{\infty 2}$. Similar expressions for the cross-spectra $\Theta_{22}$, $\Theta_{33}$ and $\Theta_{12}$ can be found. We concentrate in more detail on the spectra at one point. Then

$$\Theta_{11}(\mathbf{x}; K_1) = \Theta_{\infty 11}(K_1) + I_{A1}(\mathbf{X}; K_1) + I_{B1}(\mathbf{X}; K_1), \quad (2.53a)$$

where

$$I_{A1} = iK_1 \int_{-\infty}^{\infty}\int_{-\infty}^{\infty} \frac{[\exp\{i(-K_2\, Y)\}\, \Phi_{\infty 12} - \exp\{iK_2\, Y\}\, \Phi_{\infty 21}]}{(K_1^2+K_3^2)^{\frac{1}{2}}} \times \exp\{-(K_1^2+K_3^2)^{\frac{1}{2}} Y\}\, dK_2\, dK_3 \quad (2.53b)$$

and

$$I_{B1} = K_1^2 \int_{-\infty}^{\infty}\int_{-\infty}^{\infty} \frac{\exp\{-2(K_1^2+K_3^2)^{\frac{1}{2}} Y\}\, \Phi_{\infty 22}\, dK_2\, dK_3}{K_1^2+K_3^2}. \quad (2.53c)$$

Similarly

$$\Theta_{33}(\mathbf{X}; K_1) = \Theta_{\infty 33}(K_1) + I_C + I_D, \quad (2.54a)$$

where

$$I_C = i \int_{-\infty}^{\infty}\int_{-\infty}^{\infty} \frac{K_3}{(K_1^2+K_3^2)^{\frac{1}{2}}} [\exp\{i(-K_2\, Y)\}\, \Phi_{\infty 32} - \exp\{iK_2\, Y\}\, \Phi_{\infty 23}] \times \exp\{-(K_1^2+K_3^2)^{\frac{1}{2}} Y\}\, dK_2\, dK_3 \quad (2.54b)$$

and

$$I_D = \int_{-\infty}^{\infty}\int_{-\infty}^{\infty} \frac{K_3^2}{K_1^2+K_3^2} \exp\{-2(K_1^2+K_3^2)^{\frac{1}{2}} Y\}\, \Phi_{\infty 22}\, dK_2\, dK_3. \quad (2.54c)$$

Also,

$$\Theta_{22}(\mathbf{X}; K_1) = \int_{-\infty}^{\infty}\int_{-\infty}^{\infty} [1 - 2\cos(K_2\, Y) \exp\{-(K_1^2+K_3^2)^{\frac{1}{2}} Y\} + \exp\{-2(K_1^2+K_3^2)^{\frac{1}{2}} Y\}] \times \Phi_{\infty 22}\, dK_2\, dK_3. \quad (2.55)$$

These results for the one-dimensional spectra in the source layer $B^{(s)}$ (when $x \gg L_\infty$) are independent of the form of the energy spectrum tensor of the free-stream turbulence $\Phi_{\infty ij}$, and give rise to some general conclusions about the turbulence in region $B^{(s)}$.

First, of course (2.55) shows that $\Theta_{22}(K_1) = 0$ on $Y = 0$. Since

$$\sum_{i=1}^{3} K_i\, \Phi_{\infty ij} = \sum_{j=1}^{3} K_j\, \Phi_{\infty ij} = 0$$

for any homogeneous turbulence (Batchelor 1953), it follows from (2.53)–(2.55) that

$$\Theta_{11}(K_1) + \Theta_{33}(K_1) = \sum_{i=1}^{3} \Theta_{\infty ii}(K_1) \quad \text{as} \quad Y \to 0, \quad (2.56a)$$

so that as $Y \to 0$

$$\int_{-\infty}^{\infty} \sum_{i=1}^{3} \Theta_{ii}(K_1)\, dK_1 = \overline{u_1^2} + \overline{u_3^2} = \overline{q^2} = \overline{u_{\infty 1}^2} + \overline{u_{\infty 2}^2} + \overline{u_{\infty 3}^2} = \overline{q_\infty^2}. \quad (2.56b)$$

This means that, just outside the viscous boundary layer $B^{(v)}$ on the moving wall, the kinetic energy of the turbulence (for all directions) at each frequency is the same as that in the free stream and therefore the total kinetic energy is the same. Equally significant is that when $Y \neq 0$ the total kinetic energy is *not* necessarily the same as in the free stream.

If the free-stream turbulence is isotropic, then

$$\overline{u_1^2} = \overline{u_3^2} = 1{\cdot}5\,\overline{u_{\infty 1}^2}, \quad \overline{u_2^2} = 0 \quad \text{as} \quad Y \to 0. \tag{2.57}$$

If the turbulence in the free stream is anisotropic, then depending on the ratio of $\overline{u_{\infty 1}^2}$ to $\overline{u_{\infty 2}^2}$, in principle $\overline{u_1^2}/\overline{u_{\infty 1}^2}$ can range from 0 to $\omega$. Only (2.56*b*) must be satisfied.

It is also interesting to note the general forms of the spectra at very low and very high frequencies near the wall. From (2.52), since $I_{A1} = I_{B1} = 0$ when $K_1 = 0$,

$$\Theta_{11}(K_1 = 0,\, Y) = \Theta_{\infty 11}(K_1 = 0) = 1/\pi. \tag{2.58}$$

Therefore if the local Eulerian integral time and length scales are $T_1$ and ${}^xL_1$ respectively, where

$$T_1 = \frac{1}{(u_1')^2}\int_0^\infty \overline{u_1'(t)\,u_1'(t+\tau)}\,d\tau$$

and

$${}^xL_1 = \bar{u}T_1,$$

then from (2.56*b*)

$$T_1 = T_{\infty 1}(\overline{u_1^2}(Y)/\overline{u_{\infty 1}^2})^{-1}, \quad {}^xL_1 = L_\infty(\overline{u_1^2}(Y)/\overline{u_{\infty 1}^2})^{-1} \quad \text{as} \quad Y \to 0. \tag{2.59}$$

Therefore for isotropic turbulence $T_1(Y \to 0) = \frac{2}{3}T_{\infty 1}$ and ${}^xL_1(Y \to 0) = \frac{2}{3}L_\infty$ where $T_{\infty 1}$ is the value of $T_1$ in the free stream. From (2.54*a*) as $Y \to 0$, it can be shown that since the turbulence is homogeneous

$$\Theta_{33}(K_1 \to 0) = T_{\infty 3}/(\pi T_{\infty 1}) + \Theta_{\infty 22} \quad (K_1 \to 0), \tag{2.60a}$$

where $T_{\infty 3}$ is defined for $u_3'$ just as $T_{\infty 1}$ is for $u_1'$. For isotropic turbulence $T_{\infty 3}/T_{\infty 1} = \frac{1}{2}$ and $\Theta_{\infty 22}(K_1 \to 0) = 1/2\pi$, so that

$$\left.\begin{aligned} &\Theta_{33}(K_1 \to 0) = 1/\pi = 2\Theta_{\infty 33} \quad (K_1 \to 0), \\ \text{and} \qquad &{}^xL_3 = 2{}^xL_{\infty 3} = L_\infty. \end{aligned}\right\} \tag{2.60b}$$

So, whereas the low frequency spectrum of $u_1$ is unaffected by the wall, the spectrum of $u_3$ is amplified most at low frequencies.

The variation of $\Theta_{ij}$ and $\overline{u_i^2}$ through the region $B^{(s)}$ depends on the form of $\Phi_{\infty lm}$ and thence $\Theta_{\infty 11}$. We consider two expressions appropriate to isotropic grid turbulence, both having the same form:

$$\Theta_{\infty 11} = g_1/[g_2 + K_1^2]^\mu \tag{2.61}$$

with

$$\Phi_{\infty lm} = g_3[K^2\delta_{lm} - K_l K_m]/[g_2 + K^2]^{\mu+2} \quad (K^2 = K_i K_i). \tag{2.62}$$

In the von Kármán form [see Hunt 1973, equations (6.5), (6.7)]

$$\mu = \tfrac{5}{6}, \quad g_1 = 0{\cdot}1955, \quad g_2 = 0{\cdot}558, \quad g_3 = 55g_1/(36\pi) \tag{2.63}$$

while in the form used by Townsend (1976, p. 107)

$$\mu = 1, \quad g_1 = 1/\pi_1 \quad g_2 = 1, \quad g_3 = 2g_1/\pi. \tag{2.64}$$

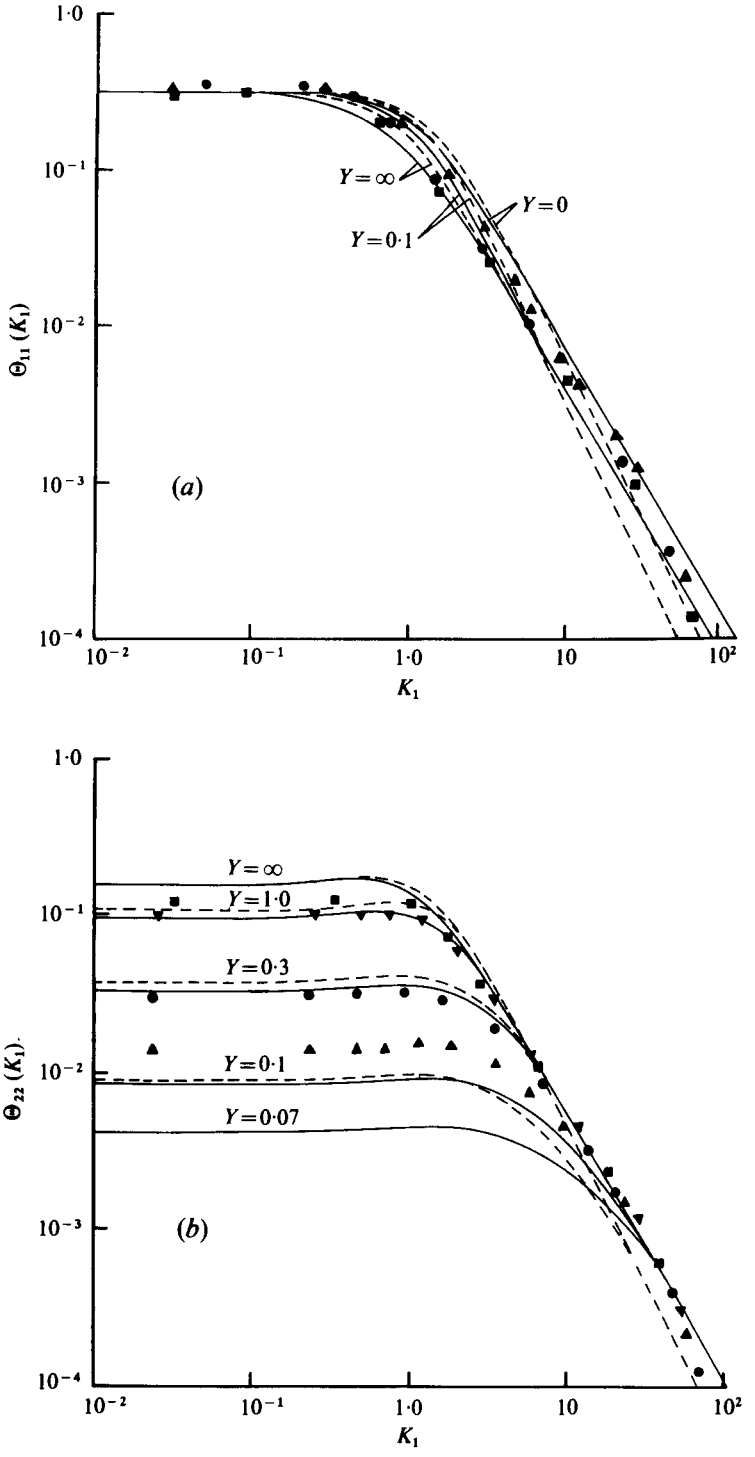


FIGURES 2(*a*, *b*). For caption see page 224.

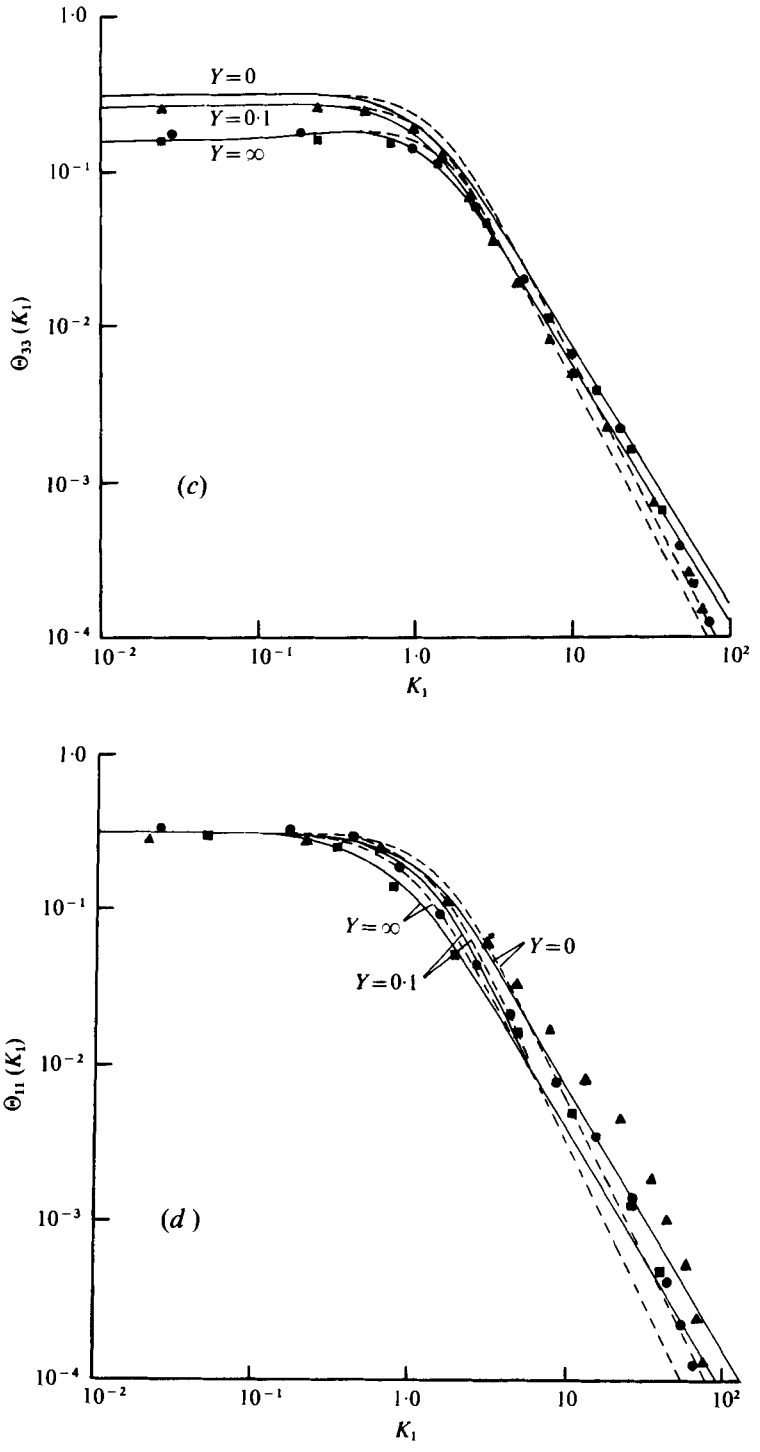


FIGURES 2 (*c*, *d*). For caption see page 224.

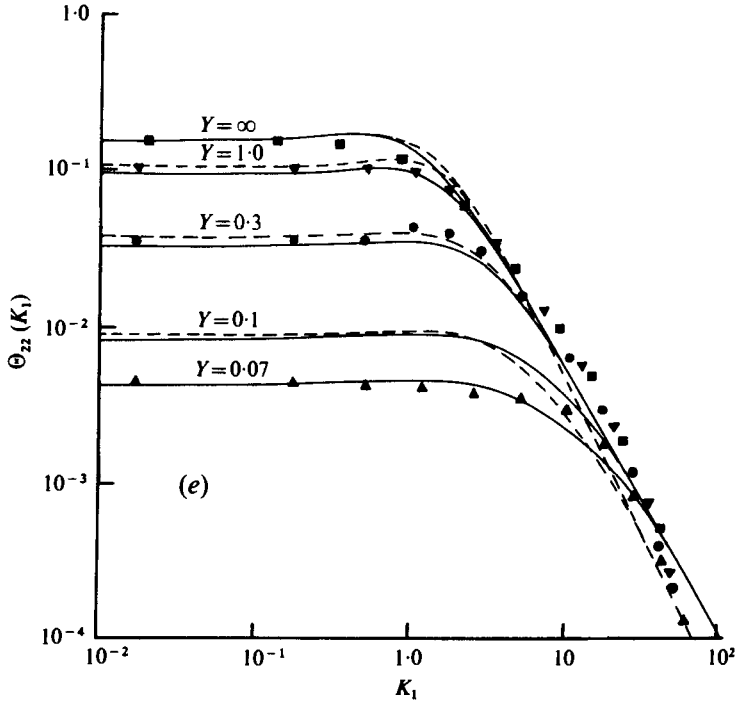


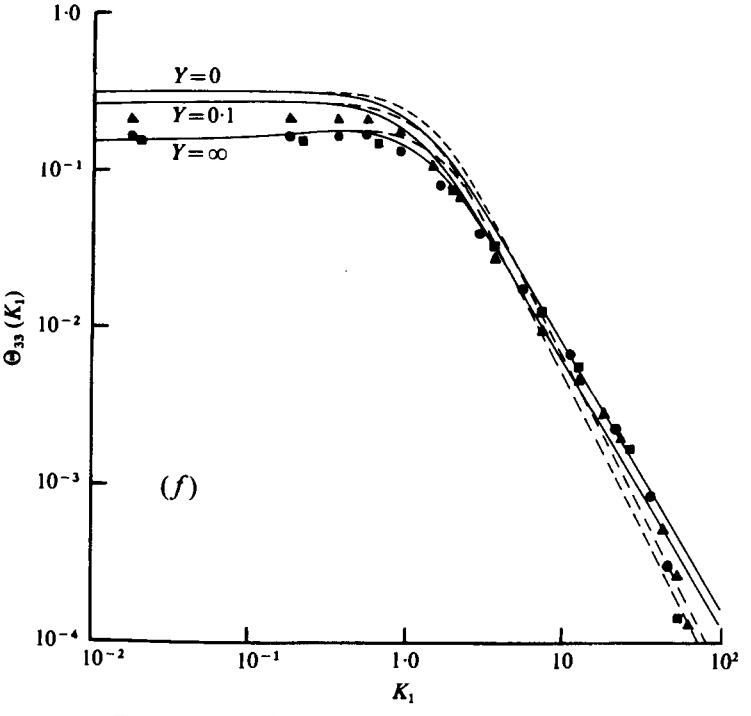


FIGURES 2(e, f). For caption see page 224.

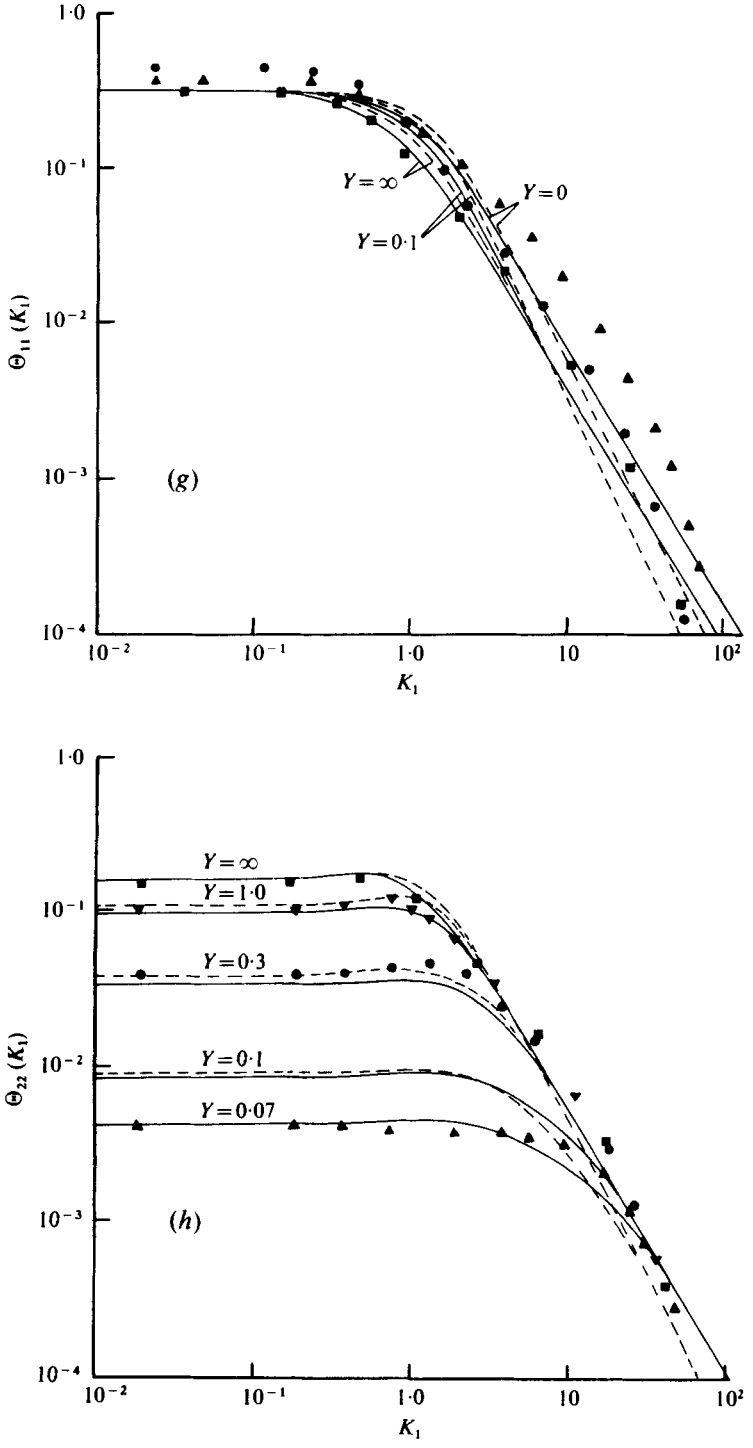


FIGURES 2(*g*, *h*). For caption see page 224.

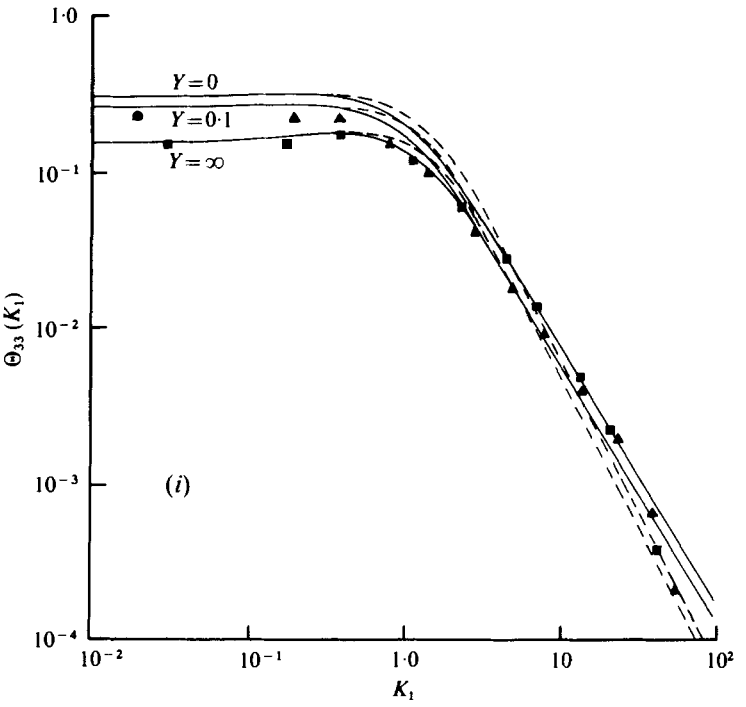


FIGURE 2. One-dimensional (power) spectra in region $B^{(a)}$ computed for two types of spectrum of free-stream turbulence compared with experimental data from Thomas & Hancock (1977) ($Y = y/L_\infty$). ——, $\mu = \frac{5}{6}$, – – –, $\mu = 1$. (*a*) Streamwise component, $(x-x_g)/M = 13$. Measured: ▲, $Y = 0{\cdot}111$; ●, $Y = 0{\cdot}251$; ■, $Y = 1{\cdot}63$. (*b*) Normal component, $(x-x_g)/M = 13$. Measured: ▲, $Y = 0{\cdot}207$; ●, $Y = 0{\cdot}319$; ▼, $Y = 1{\cdot}06$; ■, $Y = 2{\cdot}04$. (*c*) Spanwise component, $(x-x_g)/M = 13$. Measured: ▲, $Y = 0{\cdot}138$; ●, $Y = 0{\cdot}314$; ■, $Y = 1{\cdot}60$. (*d*) Streamwise component, $(x-x_g)/M = 18$. Measured: ▲, $Y = 0{\cdot}057$; ●, $Y = 0{\cdot}256$; ■, $Y = 2{\cdot}84$. (*e*) Normal component, $(x-x_g)/M = 18$. Measured: ▲, $Y = 0{\cdot}071$; ●, $Y = 0{\cdot}321$; ▼, $Y = 0{\cdot}843$; ■, $Y = 3{\cdot}57$. (*f*) Spanwise component, $(x-x_g)/M = 18$. Measured: ▲, $Y = 0{\cdot}071$; ●, $Y = 0{\cdot}371$; ■, $Y = 2{\cdot}67$. (*g*) Streamwise component, $(x-x_g)/M = 25$. Measured: ▲, $Y = 0{\cdot}080$; ●, $Y = 0{\cdot}283$; ■, $Y = 2{\cdot}72$. (*h*) Normal component, $(x-x_g)/M = 25$. Measured: ▲, $Y = 0{\cdot}079$; ●, $Y = 0{\cdot}349$; ▼, $Y = 0{\cdot}987$; ■, $Y = 3{\cdot}36$. (*i*) Spanwise component, $(x-x_g)/M = 25$. Measured: ▲, $Y = 0{\cdot}099$; ■, $Y = 3{\cdot}36$.

Graphs of the one-dimensional spectra are plotted for different values of $Y$ in figure 2. Note how the maximum value of $\Theta_{11}$ at $Y = 0$ is at a value of $K_1$ ($= 2\pi n L_\infty/\bar{u}_\infty$) of about 1·0 and *not* at $K_1 = 0$, whereas the maximum value of $\Theta_{33}$ at $Y = 0$ is at $K_1 = 0$ and is equal to $1/\pi$, which is twice its value in the free stream, in agreement with (2.60*b*).

As $Y \to 0$, if $K_1$ is $O(1)$ then $\Theta_{22}(K_1) \to 0$. But if $K_1$ is large compared with $Y^{-1}$ as $Y \to 0$, then $\Theta_{22}(K_1)$ remains equal to $\Theta_{\infty 22}(K_1)$. The asymptotic form for $\Theta_{22}(K_1)$ can be found directly from the integral (2.64*b*) by the methods explained in Hunt (1973, §6).

When $Y \to 0$ and $K_1 \to 0$, $\Theta_{22}(K_1) \sim \gamma Y^{\frac{5}{3}}$, where

$$\gamma = \frac{2g_1\,\Gamma(\frac{1}{3})}{\Gamma(\frac{5}{6})}\left[\frac{9}{5}\frac{2^{\frac{2}{3}}}{\pi^{\frac{1}{2}}}\Gamma(\tfrac{7}{3}) - \frac{1}{\Gamma(\frac{7}{6})}\right] = 0{\cdot}77 \tag{2.65}$$

for the von Kármán spectrum, for which $\mu = \frac{5}{6}$. Thus, as $Y \to 0$ and $K_1 \to 0$,

$$\Theta_{22}(K_1)/\Theta_{\infty 22}(K_1) \sim 0{\cdot}77(2\pi)\,Y^{\frac{5}{3}} = 4{\cdot}8\,Y^{\frac{5}{3}}. \tag{2.66}$$

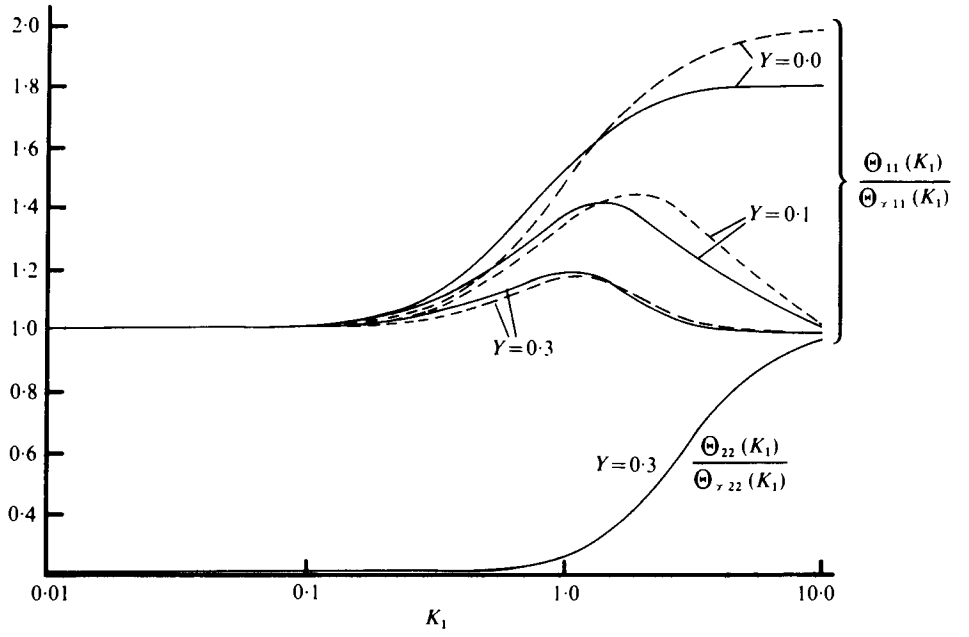


FIGURE 3. Amplification of spectra near the wall, expressed as the ratios $\Theta_{11}(K_1)/\Theta_{\infty 11}(K_1)$ and $\Theta_{22}(K_1)/\Theta_{\infty 22}(K_1)$, for various values of $Y$ ($= y/Lx$). ——, $\mu = \frac{5}{6}$; – – –, $\mu = 1$.

As $K_1$ increases $\Theta_{22}(K_1)/\Theta_{\infty 22}(K_1)$ increases, so (2.63) gives the lowest value of this ratio.

In figure 3 the amplification $\Theta_{11}/\Theta_{\infty 11}$ has been plotted as a function of $K_1$ for various values of $Y$ and for two values of $\mu$. Note that the maximum amplification occurs at a wavenumber $K_1$ given approximately by $K_1 Y \simeq 0{\cdot}3$ (for $\mu = \frac{5}{6}$), so that as $Y \to 0$ the maximum amplification occurs as $K_1 \to \infty$. Note that the amplification is only weakly dependent on $\mu$. For example, at $Y = 0{\cdot}1$ the maximum amplification is 1·45 for $\mu = 1$ and 1·43 for $\mu = \frac{5}{6}$.

The mean-square turbulent velocities are obtained by integrating $\Theta_{11}$, $\Theta_{22}$ and $\Theta_{33}$ with respect to $K_1$. These integrals have been computed and $\overline{u_1^2}(Y)$ and $\overline{u_i^2}(Y)$ are plotted in figure 4. Asymptotic expansions for $\overline{u_1^2}$ and $\overline{u_2^2}$ can be obtained near the bottom of the region $B^{(s)}$.

For the von Kármán spectrum ($\mu = \frac{5}{6}$), as $Y \to 0$

$$\overline{u_1^2}/\overline{u_{\infty 1}^2} = \overline{u_3^2}/\overline{u_{\infty 3}^2} = 1{\cdot}5 - \lambda_1 Y^{\frac{2}{3}}, \tag{2.67}$$

$$\overline{u_2^2}/\overline{u_{\infty 2}^2} = \lambda_2 y^{\frac{2}{3}}, \tag{2.68}$$

$$\lambda_1 = g_1\left\{\frac{\Gamma(\frac{7}{3})\,\Gamma(\frac{1}{3})}{\Gamma(\frac{5}{6})}\,3\pi^{\frac{1}{2}}2^{-\frac{1}{3}} + \frac{\pi\Gamma(\frac{1}{3})}{4\Gamma(\frac{5}{6})\,\Gamma(\frac{13}{6})}\right\} = 2{\cdot}68, \quad \lambda_2 = 1{\cdot}4.$$

For the 'Townsend' spectrum ($\mu = 1$)

$$\overline{u_1^2}/\overline{u_{\infty 1}^2} = 1{\cdot}5 - O(y), \tag{2.69a}$$

and

$$\overline{u_2^2}/\overline{u_{\infty 2}^2} = O(y). \tag{2.69b}$$

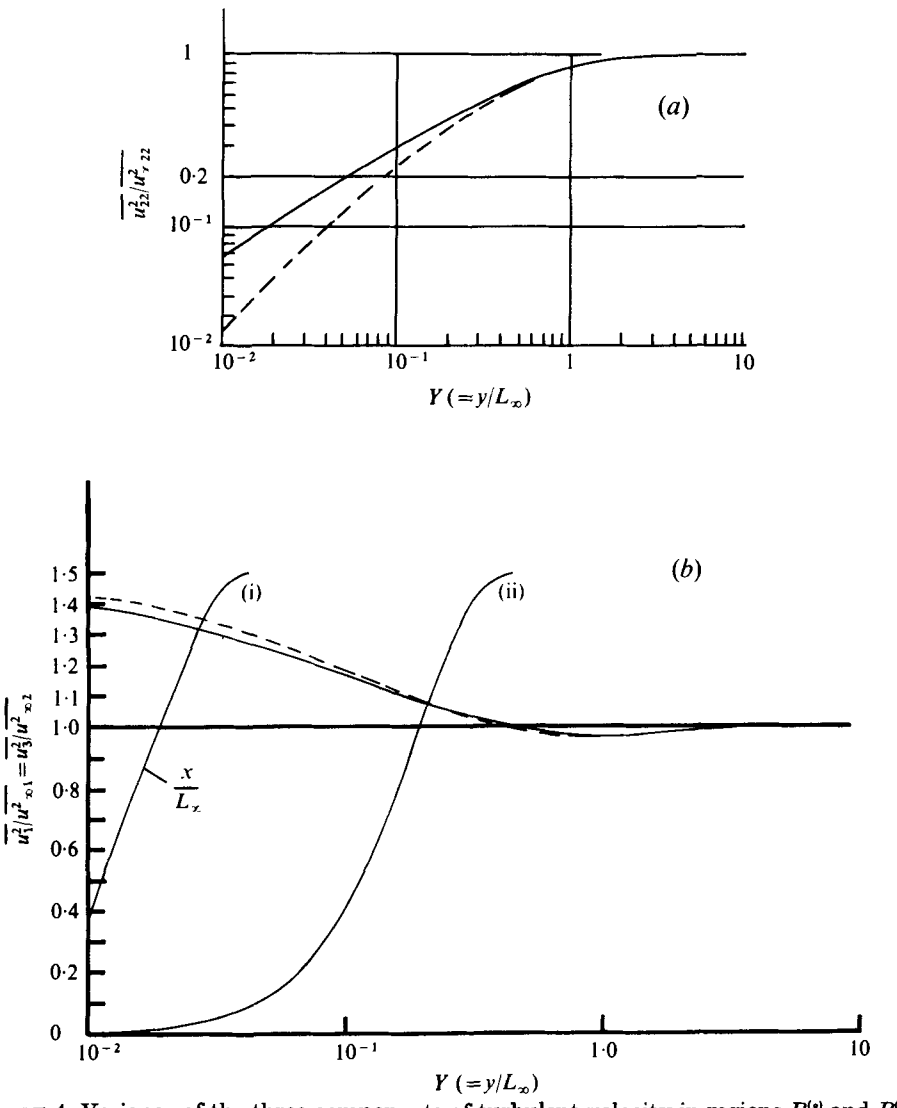


FIGURE 4. Variance of the three components of turbulent velocity in regions $B^{(s)}$ and $B^{(v)}$ for two types of free-stream turbulence spectrum. In $B^{(s)}$: ——, $\mu = \frac{5}{6}$; – – –, $\mu = 1$. In $B^{(v)}$: (i) $\mu = \frac{5}{6}$, $(x/L_\infty)\,(\nu/\bar{u}_\infty L_\infty) = 10^{-4}$; (ii) $\mu = \frac{5}{6}$, $(x/L_\infty)\,(\nu/\bar{u}_\infty L\bar{u}_\infty) = 10^{-2}$. (*a*) Normal component $\overline{u_2^2}$; note log–log scale. (*b*) Streamwise ($\overline{u_1^2}$) and spanwise ($\overline{u_3^2}$) components; note linear–log scale.

Given (2.67) or (2.69*a*), $\overline{u_1^2}$ and $\overline{u_3^2}$ in region $B^{(v)}$ can be calculated from (2.37). The results are shown in figure 4 (*b*) for two values of $x\nu/\bar{u}_\infty$. Figure 4 (*b*) shows graphically how the more energy there is in the spectrum at high wavenumbers the greater $\overline{u_2^2}$ is near $Y = 0$ (i.e. $\overline{u_2^2}$ is greater near $Y = 0$ when $\mu = \frac{5}{6}$ than when $\mu = 1$). This is fairly obvious since the more energy there is in the smallest eddies, the less the turbulence is affected by the wall.

From (2.67) and (2.59), we find that the integral scale of the streamwise velocity component is (for $\mu = \frac{5}{6}$) $\qquad {}^xL_1 = L_\infty/(1{\cdot}5 - 2{\cdot}4\,Y^{\frac{5}{6}})$,

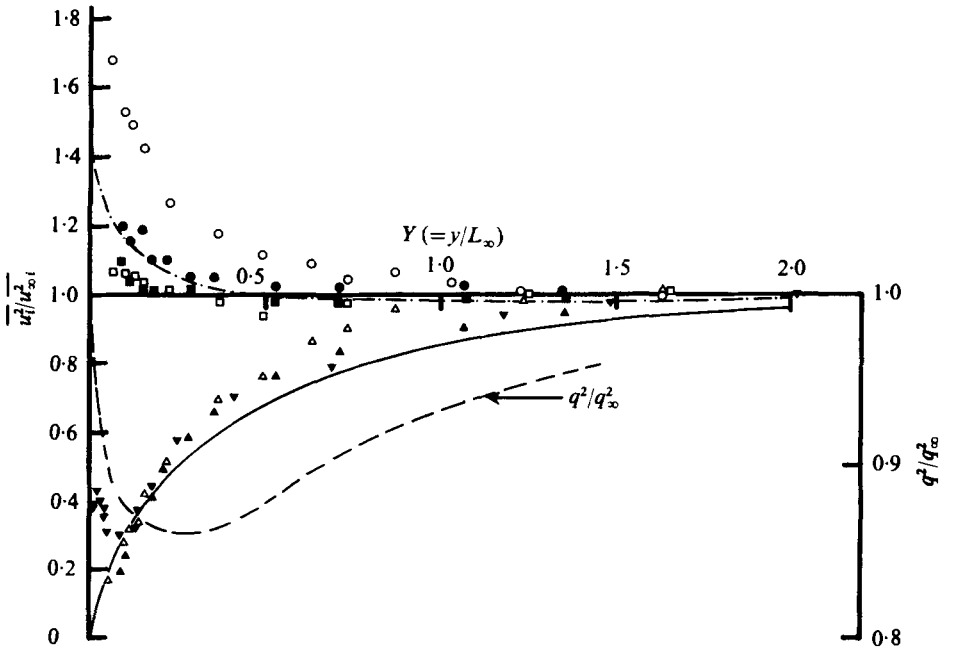


FIGURE 5. Variance of the turbulence components and the turbulent energy in region $B^{(a)}$. Linear graph. Theory: —·—, $\overline{u_1^2}/\overline{u_{\infty 1}^2} = \overline{u_3^2}/\overline{u_{\infty 3}^2}$; ——, $\overline{u_2^2}/\overline{u_{\infty 2}^2}$; – –, $\overline{q^2}/\overline{q_\infty^2}$ $(\overline{q^2} = \overline{u_1^2} + \overline{u_2^2} + \overline{u_3^2})$.

| | $(x-x_g)/M = 18$ | $(x-x_g)/M = 13$ | $x/M = 4$ |
|---|---|---|---|
| $\overline{u_1^2}/\overline{u_{\infty 1}^2}$ | ○ | ● | |
| $\overline{u_2^2}/\overline{u_{\infty 2}^2}$ | △ | ▲ | ▼ |
| $\overline{u_3^2}/\overline{u_{\infty 3}^2}$ | □ | ■ | |
| source | Thomas & Hancock (1977) | | Graham (1976) |

so that near the surface the integral scale increases very rapidly as $Y$ increases, a phenomenon observed in many turbulent flows near surfaces as we note later.

From (2.65) and (2.68), we find that the streamwise integral scale of the vertical velocity component is (for $\mu = \frac{5}{6}$)

$$^xL_2 = \pi\Theta_{22}(0)/\overline{u_2^2} = \pi Y^{\frac{5}{3}}/\lambda_2\, Y^{\frac{2}{3}} = 2{\cdot}24\,Y.$$

$^xL_2$ is also proportional to $Y$ for the other spectrum, with $\mu = 1$. This result is found in many turbulent flows where the precise conditions of this theory are not satisfied.

It is also interesting to consider how as $Y$ increases $\overline{u_1^2}$ and $\overline{u_2^2}$ approach their asymptotic values in the free-stream turbulence. Figure 4 shows that $\overline{u_1^2}$ and $\overline{u_3^2}$ first decrease to values *below* $\overline{u_{\infty 1}^2}$ and $\overline{u_{\infty 3}^2}$ before increasing to their asymptotic values. The lowest they reach for $\mu = \frac{5}{6}$ is $0{\cdot}865\overline{u_{\infty 1}^2}$ and for $\mu = 1$ is $0{\cdot}845\overline{u_{\infty 1}^2}$. The asymptotic form of $\overline{u_1^2}$ or $\overline{u_3^2}$ as $Y \to \infty$ is

$$\overline{u_1^2}/\overline{u_{\infty 1}^2} = \overline{u_3^2}/\overline{u_{\infty 3}^2} = 1 - \lambda_3\, Y^{-\frac{7}{6}} e^{-0{\cdot}74Y} + O(Y^{-4}) \quad \text{for} \quad \mu = \tfrac{5}{6},$$

where $\lambda_3 = \pi g_1/[2^{\frac{1}{3}}\Gamma(\frac{5}{6})\, g_2^{\frac{11}{12}}] = 0{\cdot}525$. Thus $\overline{u_1^2}$ is *less* than $\overline{u_{\infty 1}^2}$ for $0{\cdot}5 < Y \lesssim 0{\cdot}8$ and then very slightly increases above $\overline{u_{\infty 1}^2}$. On the other hand $\overline{u_2^2}$ effectively increases

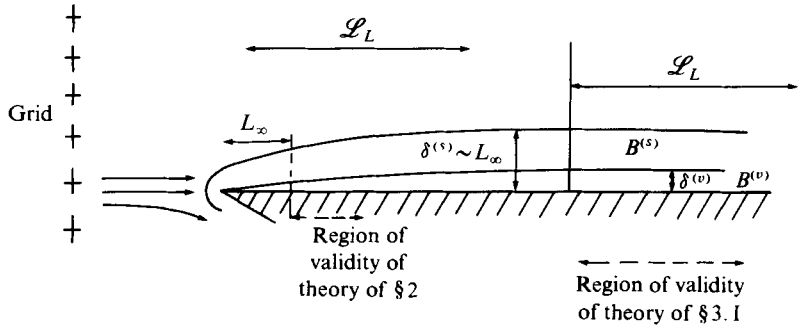


FIGURE 6. Regions of validity of theories of §§2 and 3.1.

monotonically to $\overline{u^2_{\infty 2}}$ and from its asymptotic form we find that $\overline{u_2^2}$ is slightly greater than $\overline{u^2_{\infty 2}}$ for $Y \gtrsim 4$. The $Y^{-4}$ decay law as $Y \to \infty$ is the same as that found by Phillips (1955) for the decay of velocity fluctuations outside a shear layer. Note that for practical purposes $\overline{u_1^2}$ and $\overline{u_3^2}$ reach 10% of their asymptotic values when $Y(= y/L_\infty) > 0{\cdot}2$, whereas $\overline{u_2^2}$ does not reach 10% of its asymptotic value until $Y > 1{\cdot}2$.

In figure 5 we have plotted $\overline{q^2}/\overline{q^2_\infty}$ as a function of $Y$ to show how the kinetic energy of the turbulence is lower in region $B^{(s)}$ (except at $Y = 0$) than in the free stream. The lowest value this ratio reaches is 0·865 for $\alpha = \frac{5}{6}$ and 0·845 for $\alpha = 1$. The decrease in the energy of the turbulence, of course, is associated with a rise in the mean pressure. For example, when $\mathscr{L}_L \gg x \gg L_\infty$ there is a gradient of the mean pressure normal to the wall: $\partial\overline{p}/\partial y = -\partial\overline{u_2^2}/\partial y$.

## 3. Applications of the theory

### 3.1. *Grid turbulence near a moving wall*

The theory of §2 has been developed for a limited range of $x$ over which the turbulence does not decay significantly. To compare the theory with experiments we must estimate how the turbulence decays in the wall regions $B^{(s)}$ and $B^{(v)}$ relative to its decay in the free stream. The usual law for the decay of homogeneous grid turbulence is (Batchelor 1953, p. 103)

$$d\overline{q^2_\infty}/dt = -A(\overline{q^2_\infty})^{\frac{3}{2}}/l, \tag{3.1}$$

where $l$ is some scale of the order of the integral scale.

In region $B^{(s)}$, if $\delta^{(v)} \ll L_\infty$ we have found in §2.4 that $\overline{q^2} \simeq \overline{q^2_\infty}$ to within 1% and that $L_x$ decreases by a third, while the integral scale for $u_3$ increases by about a quarter. It is also interesting to note that the highest wavenumber parts of the spectrum are unaffected in region $B^{(s)}$. Thus there is no apparent reason to expect the turbulence decay in $B^{(s)}$ to differ much from that in the free stream.

Even if these two turbulence decay rates are comparable, is there any reason why $\mathbf{u}$ in $B^{(s)}$ should have the form given in §2? Consider the flow downstream when $x > x_0$ (see figure 6). We assume that although the turbulence may have travelled a distance from the grid comparable with $\mathscr{L}_L$ the thickness $\delta^{(v)}$ of the viscous region is still small compared with $L_\infty$, the local integral scale of the free stream. Let us calculate the flow

at a distance $x-x_0$ from our new origin $x_0$, where $x-x_0$ is large compared with $L_\infty$ but small compared with $\mathscr{L}_L$, in other words less than an eddy life-time away from $x_0$. In that case we can again use the concepts of 'frozen' turbulence. If the decay of turbulence in $B^{(s)}$ has been comparable with that in the free stream, then

$$\boldsymbol{\omega} \simeq \boldsymbol{\omega}_\infty \quad \text{in} \quad B^{(s)} \quad \text{for} \quad y > \delta^{(v)}, \tag{3.2}$$

so that as in (2.31) we can express $\mathbf{u}$ as

$$\mathbf{u} = \mathbf{u}_\infty - \nabla\Phi,$$

where $\nabla \times \mathbf{u} = \boldsymbol{\omega}$, $\mathbf{u} \to \mathbf{u}_\infty$ as $Y(=y/L_\infty) \to \infty$ and $\nabla^2\Phi = 0$. Let $(x-x_0)/L_\infty = X$; then on $X = 0$, $\mathbf{u}-\mathbf{u}_\infty$ must be regarded as unknown, say $\mathbf{u}_0(0, Y, Z, T)$, but as $Y \to 0$, $u_2 \to 0$, so that $\partial\Phi/\partial Y = u_{\infty 2}$. Therefore for $X > 0$

$$\begin{aligned}\Phi = &-\frac{1}{2\pi}\int_0^\infty\int_{-\infty}^\infty \frac{u_{\infty 2}(X', Y=0, Z', T)}{[(X-X')^2+Y^2+(Z-Z')^2]^{\frac{1}{2}}}\,dX'\,dZ' \\ &-\frac{1}{2\pi}\int_0^\infty\int_{-\infty}^\infty u_{01}(0, Y', Z', T)\left\{\frac{1}{[X^2+(Y-Y')^2+(Z-Z')^2]^{\frac{1}{2}}}\right. \\ &\left.+\frac{1}{[X^2+(Y+Y')^2+(Z-Z')^2]^{\frac{1}{2}}}\right\}dY'dZ'. \end{aligned} \tag{3.3}$$

Thus when $X \gg 1$ (i.e. $\mathscr{L} \gg x \gg L_\infty$), the second integral is $O(X^{-1})$ times the first. Consequently $\Phi$ and $\beta_i$ tend to the forms found in (2.34) and (2.44). Therefore we expect that the results of §2.4, when expressed in local free-stream variables, should be approximately valid down the wind tunnel.†

In comparing the theoretical results with experiments the first question to be answered is what is the relative magnitude of $\delta^{(v)}$ and $L_\infty$, the thicknesses of the viscous and source regions. From (2.37*b*)

$$\delta^{(v)}/L_\infty = 4{\cdot}0[(x/L_\infty)\,\nu/(\bar{u}_\infty L_\infty)]^{\frac{1}{2}}. \tag{3.4}$$

Since $\overline{u_1^2}/\overline{u_{\infty 1}^2}$ begins to be amplified only when $y/L_\infty < 0{\cdot}2$, it follows that if $\delta^{(v)}/L_\infty \gtrsim 0{\cdot}2$ then the irrotational amplification of the $u_1$ component of turbulence will be masked by the viscous reduction. This is why Uzkan & Reynolds (1967) observed no amplification. The Reynolds number of their experiment was so low that

$$(x/L_\infty)\,(\nu/\bar{u}_\infty L_\infty) \simeq 10^{-2}$$

(where $x$ is the distance from the beginning of the moving wall), so that $\delta^{(v)}/L_\infty \simeq 0{\cdot}4$. In their conclusions they stated that the turbulence was reduced within a growing 'inhomogeneity' layer of thickness $\delta = 1{\cdot}8(\nu x/\bar{u}_\infty)^{\frac{1}{2}}$, which is in rough agreement (1·8 compared with 4·0) with our calculations! Uzkan & Reynolds' data can be plotted within 12 % on a universal plot of $\overline{u_1^2}/\overline{u_{\infty 1}^2}$ as a function of $y/(x\nu/\bar{u}_\infty)^{\frac{1}{2}}$, showing that our solution for the viscous layer has the right form. (Note that $x < \mathscr{L}_L$.)

A possible explanation for the thickness of the viscous layer observed by Uzkan & Reynolds being less than that predicted by (3.4) is that, since in their case $\delta^{(v)} \simeq \delta^{(s)}$, the boundary-layer approximation $\delta^{(v)} \ll \delta^{(s)}$ is not valid. Then some irrotational amplification of $u_1$ must occur in the outer part of their viscous layer.

If the Reynolds number is very much higher than in Uzkan & Reynolds' experiment,

† When $\delta^{(v)} \gtrsim 0{\cdot}2L_\infty$, there is a significant quantity of vorticity diffused from $B^{(v)}$ into the source layer $B^{(s)}$. Then (3.2) and (3.3) cease to be valid.

as in the experiments of Thomas & Hancock (1977) at Imperial College, then $\delta^{(v)} \ll L_\infty$. Typically $(x/L_\infty)(\nu/\overline{u}_\infty L_\infty) \sim \frac{40}{4} \times 10^4$), so that

$$\delta^{(v)}/L_\infty \simeq 0{\cdot}1. \tag{3.5}$$

Thus from figure 4($b$) we should expect a maximum amplification in $\overline{u_1^2}/\overline{u_{\infty 1}^2}$ of about 20%. To achieve an amplification of 30% would require an increase in $\overline{u}_\infty L_\infty/\nu$ by a factor of 10.

The thickness $\delta^{(v)}$ of the viscous layer does not increase with $x$ indefinitely. The theory leading to the prediction (2.37$b$) was based on eddies travelling at the same speed as the mean flow. Over a distance $x \gtrsim \mathscr{L}_L$, the additional random convection of the eddies by the turbulence produces phase changes in the eddies travelling with the mean flow. Taking a single Fourier component provides an estimate for $\delta^{(v)}$ for $x \gtrsim \mathscr{L}_L$ of

$$\begin{aligned}\delta^{(v)} &\simeq 2[\mathscr{L}_L \nu/\overline{u}_\infty]^{\frac{1}{2}} \simeq 2[\nu L_\infty/u'_\infty]^{\frac{1}{2}} \\ &\simeq 2\,[\nu \times \text{Lagrangian time scale}]^{\frac{1}{2}}.\end{aligned} \tag{3.6}$$

This estimate is much larger than $[\nu L_\infty/\overline{u}]^{\frac{1}{2}}$, the thickness proposed for the viscous sublayer in a turbulent boundary layer by Sternberg (1962) from an analysis in which the convection of eddies was neglected and a single Fourier component was considered.

The experimental results of Thomas & Hancock (1977) for turbulence near a moving wall are compared with the theoretical curves in figures 2 and 5. The salient parameter values for their experiment are

$$u'_\infty/\overline{u}_\infty = 0{\cdot}05, \quad \overline{u}_\infty L_\infty/\nu = 10^5, \quad (\overline{u_{\infty 1}^2}/\overline{u_{\infty 2}^2})^{\frac{1}{2}} = \overline{u_{\infty 1}^2}/\overline{u_{\infty 3}^2})^{\frac{1}{2}} = 1{\cdot}09 \quad \text{at} \quad (x-x_g)/M = 18.$$

Since the boundary layer created by the rigid wall upstream of the moving wall was sucked off, the moving wall was the sole cause of the turbulence distortion near $y = 0$. The theory of § 2 should be valid for a distance $x$ from the start of the moving wall if $x \ll \mathscr{L}_\infty$. Now $\mathscr{L}_\infty$ is about 1·6 m, so when $(x-x_g)/M = 18$, $x/\mathscr{L}_L \simeq 0{\cdot}9$. Since in addition $\delta^{(v)} \ll L_\infty$ is satisfied [see (3.5)], the conditions in Thomas & Hancock's experiment approximately agree with those of our theory.

For the mean-square turbulence components in figure 5, the $\overline{u_2^2}$ data collapse well when plotted against the non-dimensional length scale $Y$ and agree well with the theoretical curve. But the $\overline{u_1^2}$ and $\overline{u_3^2}$ data both show a tendency to depart from the theoretical curve with increasing $X$, the $\overline{u_1^2}$ data showing a larger amplification and the $\overline{u_3^2}$ a correspondingly smaller one than that predicted by the theory. We think that the downstream amplification of $\overline{u_1^2}$ is due to a disturbance created at the beginning of the moving wall being diffused outwards by the turbulence.

Table 1 lists some of Thomas & Hancock's measurements of the amplification of spectra at various frequencies in the layer adjacent to the moving wall together with the corresponding values given by the theory. For $Y \simeq 0{\cdot}3$ the numerical agreement is good, but at $Y \simeq 0{\cdot}06$ the experimental values should be expected to be lower than the theoretical values because the latter have been computed on the basis of $\delta^{(v)} \simeq 0$, whereas in fact $\delta^{(v)} = 0{\cdot}1$.

In figure 2 the experimental spectra are plotted on the theoretical curves. The experimental values of $\Theta_{ii}$ and $K_1$ have been non-dimensionalized by $\overline{u_{\infty i}^2}$ and $2L_{\infty i}$ (the appropriate transverse length scale in the free stream) in the cases $i = 2$ and 3 to allow for the anisotropy of the free-stream turbulence. The measured spectrum of $\Theta_{11}$ shows

| $K_1$ | $\frac{\Theta_{22}(Y = 0{\cdot}07)}{\Theta_{22}(Y = 3{\cdot}57)}$ | | $\frac{\Theta_{11}(Y = 0{\cdot}06)}{\Theta_{11}(Y = 2{\cdot}84)}$ | | $\frac{\Theta_{33}(Y = 0{\cdot}07)}{\Theta_{33}(Y = 2{\cdot}67)}$ | |
|---|---|---|---|---|---|---|
| | Computed | Measured | Computed | Measured | Computed | Measured |
| | | $Y\ (= y/L_\infty) \simeq 0{\cdot}07$ (inside region $B^{(v)}$) | | | | |
| 0·03 | 0·027 | 0·028 | 1·02 | 0·95 | 2·0 | 1·42 |
| 0·3 | 0·026 | 0·028 | 1·11 | 1·03 | 1·73 | 1·42 |
| 1·0 | 0·033 | 0·037 | 1·45 | 1·57 | 1·34 | 1·36 |
| 3·0 | 0·11 | 0·11 | 1·45 | 1·87 | 1·12 | 0·9 |
| 10·0 | 0·43 | 0·38 | 0·96 | 2·00 | 0·99 | 0·9 |
| 30·0 | 0·89 | 0·59 | | | | |
| | | $Y \simeq 0{\cdot}3$ (inside region $B^{(s)}$) | | | | |
| 0·03 | 0·20 | 0·24 | | | | |
| 0·3 | 0·19 | 0·25 | | | | |
| 1·0 | 0·27 | 0·39 | | | | |
| 3·0 | 0·61 | 0·69 | | | | |
| 10·0 | 1·0 | 0·82 | | | | |
| 30·0 | 1·0 | 0·9 | | | | |

TABLE 1. Comparison of the values of the amplification of the spectra computed for region $B^{(s)}$ and measured by Thomas & Hancock (1977) at $(x-x_g)/M = 18$.

a bump at the high frequency end, which perhaps supports our conjecture that some disturbance was created at the upstream end of the moving wall. This bump is visible at $y/L_\infty \simeq 0{\cdot}1$, but not for $y/L_\infty > 0{\cdot}25$, so that it exists only in the viscous region.

In general the experimental data confirm the general features of the theory; i.e. the suppression of $\Theta_{22}$ as the wall is approached, which occurs mainly at the low frequency end of the spectrum, while the low frequency components of $\Theta_{11}$ remain substantially unaltered.

### 3.2. *Turbulence near a flat plate*

If a semi-infinite flat plate is placed in a turbulent flow parallel to the mean flow, then if $\delta^*$ is the displacement thickness of the boundary layer on the plate and $L_\infty \gg \delta^*$ the turbulence above the plate will be distorted. We expect that some additional turbulence may be produced in region $B^{(s)}$ by the interaction of the free-stream turbulence with the boundary layer. This is likely to be negligible as $\delta^*/L_\infty \to 0$.

Measurements undertaken at Cambridge University Engineering Department and plotted in figure 5 show that the variation of $\overline{u_2^2}/\overline{u_{\infty 2}^2}$ with $y/L_\infty$ is slightly greater than the theoretical curve for region $B^{(s)}$, by about 0·05. This difference is, we note, about equal to the value of $\delta^*/L_\infty$ (Graham 1975).

## 4. Further applications of the theory

The experiments described above, involving a moving wall or a flat plate, are rather specialized cases. A more usual situation which occurs in a wind tunnel is the growth of a tunnel wall layer in free-stream turbulence behind a grid. In this case the wall which influences the turbulence is present continuously from upstream of the origin of the turbulence and therefore may influence the homogeneity of production. There is also, usually, a relatively thick mean-flow boundary layer on the wall.

Measurements have been made in such layers by Cooke (1971) and Petty (unpublished), among others. These measurements show qualitatively some of the main features predicted by the theory of §2, in particular the decrease in $\overline{u_2^2}$ and small increase in $\overline{u_1^2}$ within the region $B^{(s)}$.

The most common occurrence of turbulent flow adjacent to a wall is within turbulent boundary layers. Bradshaw (1967) and Townsend (1976) have described the large-scale inactive motions in the inner part of a turbulent boundary layer, which are produced by the large eddies in the outer part of the boundary layer. These eddies are convected and distorted by the mean velocity shear, but are also subject to the same blocking action at the solid boundary as are the eddies of free-stream turbulence adjacent to a wall. It is therefore to be expected that some of the details of free-stream turbulence close to a wall predicted by the theory of §2 should also apply approximately to the inactive motions in turbulent boundary layers. This speculation will not be taken further here, but we believe that the theory has useful implications in this context.

## 5. Conclusions

The theory presented in §2 gives a good prediction of the variation of $\overline{u_2^2}$ and its spectrum in the region of a solid wall, when compared with measurements on a moving wall or a thin flat plate at moderately high Reynolds numbers. The numerical agreement of the $u_1$ and $u_3$ components, particularly their variances, is not so good, although qualitatively correct. In particular, the measured values of these quantities indicate a streamwise development of the wall layer giving increasing amplification of $\overline{u_1^2}$ with increasing $x/L_\infty$. The measured values of $\overline{u_3^2}$ show less amplification than is predicted by the theory.

At lower Reynolds numbers, the relatively greater predicted thickness of the viscous layer $B^{(v)}$ explains why the data of Uzkan & Reynolds show no amplification near the wall.

We are grateful to Mr P. Bradshaw for comments on a draft of this paper. The computing was ably performed by Mr J. Smith.

## Appendix A. Solution for the potential near the origin of $B^{(s)}$

The potential $\Phi$ satisfies

$$\nabla^2\Phi = 0, \tag{A 1}$$

together with the boundary conditions

$$\left.\begin{aligned} \partial\Phi/\partial Y &= u_{\infty 2} \quad \text{on} \quad Y = 0, \quad X \geqslant 0, \\ \Phi &= 0 \quad \text{on} \quad Y = 0, \quad X < 0, \\ \Phi &\to 0 \quad \text{on} \quad Y \to +\infty. \end{aligned}\right\} \tag{A 2}$$

Taking Fourier transforms defined as in (2.38) and (2.41) and substituting in (A 1) and (A 2) gives the following equations for the potential function $\beta_2(X, Y)$:

$$\partial^2\beta_2/\partial X^2 + \partial^2\beta_2/\partial Y^2 - K_3^2\beta_2 = 0, \tag{A 3}$$

$$\left.\begin{aligned} \partial\beta_2/\partial Y &= \exp(iK_1X) \quad \text{on} \quad Y = 0, \quad X \geqslant 0, \\ \beta_2 &= 0 \quad \text{on} \quad Y = 0, \quad X < 0. \end{aligned}\right\} \tag{A 4}$$

If we express $\beta_2$ as the Fourier transform

$$\int_{-\infty}^{\infty} \tilde{\beta}(\lambda, Y)\, e^{i\lambda x}\, d\lambda$$

and substitute this into (A 3), taking the appropriate solution to give $\beta_2 \to 0$ as $Y \to +\infty$, we obtain

$$\tilde{\beta}(\lambda, Y) = F(\lambda) \exp\{-(\lambda^2 + K_3^2)^{\frac{1}{2}} Y\} \quad \text{in} \quad Y \geqslant 0.$$

Hence from (A 4)

$$\int_{-\infty}^{\infty} F(\lambda)\,(\lambda^2 + K_3^2)^{\frac{1}{2}} \exp(i\lambda X)\, d\lambda = \exp(iK_1 X) \quad \text{for} \quad X \geqslant 0$$

and

$$F(\lambda) \exp(i\lambda X)\, d\lambda = 0 \quad \text{for} \quad X < 0.$$

The solution of this pair of integral equations, by consideration of the analytic continuation of $F$ in the complex $\lambda$ plane, is

$$F(\lambda) = \frac{i}{2\pi(K_1 + iK_3)^{\frac{1}{2}}(\lambda - iK_3)^{\frac{1}{2}}(\lambda - K_1)} - \frac{\delta(\lambda - K_1)}{2(K_1 + iK_3)^{\frac{1}{2}}(\lambda - iK_3)^{\frac{1}{2}}}.$$

From this

$$\beta_2(X, Y) = \frac{i}{\pi}\int_{-\infty}^{\infty} \frac{\exp\{-(\lambda^2 + K_3^2)^{\frac{1}{2}} Y\} \exp(i\lambda X)\, d\lambda}{(K_1 + iK_3)^{\frac{1}{2}}(\lambda - iK_3)^{\frac{1}{2}}(\lambda - K_1)} - \frac{\exp\{-(K_1^2 + K_3^2)^{\frac{1}{2}} Y\} \exp(iK_1 X)}{2(K_1^2 + K_3^2)^{\frac{1}{2}}}.$$

This integral can be evaluated on the wall $Y = 0$, $X \geqslant 0$ to give

$$\beta_2(X, 0) = \frac{-\operatorname{erf}\{[(iK_1 + K_3)X]^{\frac{1}{2}}\}}{(K_1^2 + K_3^2)^{\frac{1}{2}}} \exp(iK_1 X),$$

which can be expanded for large values of $X$ as

$$\beta_2(X, 0) = -\frac{\exp(iK_1 X)}{(K_1^2 + K_3^2)^{\frac{1}{2}}} + \frac{\exp(-|K_3|X)\,(K_3 - iK_1)^{\frac{1}{2}} X^{-\frac{1}{2}}}{\pi^{\frac{1}{2}}(K_1^2 + K_3^2)} + O(\exp(-|K_3|X)\, X^{-\frac{3}{2}}).$$

## Appendix B. The thickness of region $B^{(v)}$

We develop here a model for estimating the thickness of region $B^{(v)}$ at distances from the leading edge of a plate or a moving wall of the order of the eddy turnover distance $\mathscr{L}_L$. From (2.28) the normalized equation for $u_i^{(v)}$ is

$$\frac{\partial u_1^{(v)}}{\partial t} + \frac{\partial u_1^{(v)}}{\partial X} = \frac{\partial^2 u_1^{(v)}}{\partial \eta^2}, \tag{B 1}$$

with boundary conditions

$$\left.\begin{aligned} u_1^{(v)} &\to 0 \quad \text{as} \quad \eta \to \infty, \\ u_1^{(v)} &= -(u_{\infty 1} + u_1^{(s)})\,(X, Y = 0, Z, T) \quad \text{on} \quad \eta = 0, \quad X > 0, \\ u_1^{(v)} &= 0 \quad \text{on} \quad \eta = 0, \quad X < 0. \end{aligned}\right\} \tag{B 2}$$

As a simple model consider a single Fourier component, travelling with the mean flow but slowly varying in phase. A model of such a disturbance is

$$(u_{\infty 1} + u_1^{(s)})\,(Y = 0) = u_0 \cos(K_1 T - (K_1 + \delta K_1) X), \tag{B 3}$$

where $u_0$ is a constant $O(1)$, $\delta K_1 = \alpha f((T-X)/\alpha)$ and $\alpha = u'_\infty/\bar{u}_\infty$ ($\ll 1$). $f$ is a random function $O(1)$ which is constant for an observer travelling with the mean flow and which has a dimensional time scale of the order of the Lagrangian time scale, since

$$(T-X)/\alpha = (t-x)\,\bar{u}_\infty L_\infty/u'_\infty.$$

Thus the boundary conditions for $u_1^{(v)}$ are specified in terms of functions of $T-X$ and $X$. Let $u_1^{(v)}(X,\eta,Z,T) = \hat{u}_1^{(v)}(X,\eta,Z,\hat{T})$, where $T-X=\hat{T}$. Then (B 1) becomes

$$\partial\hat{u}_1^{(v)}/\partial X = \partial^2\hat{u}_1^{(v)}/\partial\eta^2 \tag{B 4}$$

and (B 2) and (B 3) become

$$\hat{u}_1^{(v)} \to 0 \quad \text{as} \quad n\to\infty,$$

$$\hat{u}_1^{(v)} = u_0\cos(K_1\hat{T}+\alpha X f(\hat{T}/\alpha)) \quad \text{as} \quad \eta\to 0. \tag{B 5}$$

The asymptotic solutions are as follows

(i) When $\alpha X(=x/\mathscr{L}_L) \ll 1$,

$$\hat{u}_1^{(v)} = u_0\cos(K_1\hat{T})\operatorname{erf}\{\eta/(4X)^{\frac{1}{2}}\},$$

or

$$u_1^{(v)} = u_0\cos(K_1(\bar{u}_\infty t-x)/L_\infty)\operatorname{erf}\{y(4\nu x/\bar{u}_\infty)^{-\frac{1}{2}}\}, \tag{B 6}$$

which is of the form of (2.37).

(ii) When $\alpha X(=x/\mathscr{L}_L) = O(1)$,

$$u_1^{(v)} = u_0\cos\{K_1\hat{T}+\alpha X f(\hat{T}/\alpha)-\eta(\tfrac{1}{2}\alpha f)^{\frac{1}{2}}\}\exp\{-\eta[\tfrac{1}{2}\alpha f(\hat{T}/\alpha)]^{\frac{1}{2}}\},$$

or

$$u_1^{(v)} = u_0\cos\{K_1(\bar{u}_\infty t-x)/L_\infty+(\alpha x/L_\infty)f(\bar{u}_\infty t-x)/\mathscr{L})-y[f(2\mathscr{L}_L\nu/\bar{u}_\infty)^{-1}]^{\frac{1}{2}}\}$$
$$\times\exp\{-[y(2\nu/\bar{u}_\infty)^{-1}][f(\bar{u}_\infty t-x)/\mathscr{L}]^{\frac{1}{2}}\}. \tag{B 7}$$

Since $f$ is assumed to be $O(1)$, it follows from (B 6) and (B 7) that the thickness $\delta^{(v)}$ of the viscous region $B^{(v)}$ near the wall changes from $4(\nu x/\bar{u}_\infty)^{\frac{1}{2}}$ when $x \ll \mathscr{L}_L$ to about $2(\mathscr{L}_L\nu/\bar{u}_\infty)^{\frac{1}{2}}$ when $x \geqslant \mathscr{L}_L$, as stated in (3.4) and (3.6) in § 3. Most other (plausible) kinds of random disturbance would produce a similar thickness when $x \gg \mathscr{L}_L$.

## REFERENCES


Batchelor, G. K. 1953 *The Theory of Homogeneous Turbulence.* Cambridge University Press.

Bradshaw, P. 1967 Inactive motion and pressure fluctuations in turbulent boundary layers. *J. Fluid Mech.* **30**, 241.

Cooke, N. J. 1971 The effect of turbulence scale on the flow around highrise building models. Ph.D. thesis, University of Bristol.

Erdélyi, A., Magnus, W., Oberhettinger, F. & Tricomi, F. G. 1954 *Tables of Integral Transforms*, vol. 1. McGraw-Hill.

Graham, J. M. R. 1976 Turbulent flow past a porous plate. *J. Fluid Mech.* **73**, 565.

Graham, J. M. R. 1975 Turbulent flow past a long flat plate. *Imp. Coll. Aero. Tech. Note* no. 75-101.

Hunt, J. C. R. 1973 A theory of flow round two-dimensional bluff bodies. *J. Fluid Mech.* **61**, 625.

Phillips, O. M. 1955 The irrotational motion outside a free boundary layer. *Proc. Camb. Phil. Soc.* **51**, 220.

STERNBERG, J. 1962 A theory for the viscous sublayer of a turbulent flow. *J. Fluid Mech.* **13**, 241.

TENNEKES, H. & LUMLEY, J. L. 1972 *A First Course in Turbulence.* M.I.T. Press.

THOMAS, N. H. & HANCOCK, P. E. 1977 Grid turbulence near a moving wall. *J. Fluid Mech.* **82**, 481.

TOWNSEND, A. A. 1961 Equilibrium layers and wall turbulence. *J. Fluid Mech.* **11**, 97.

TOWNSEND, A. A. 1976 *The Structure of Turbulent Shear Flow*, 2nd edn. Cambridge University Press.

UZKAN, T. & REYNOLDS, W. C. 1967 A shear-free turbulent boundary layer. *J. Fluid Mech.* **28**, 803.